International Journal of Engineering Science 45 (2007) 842–872

International Journal of Engineering Science

Wave scattering by a horizontal circular cylinder3 in a two-layer fluid with an ice-cover

Dilip Das, B.N. Mandal *

Physics and Applied Mathematics Unit, Indian Statistical Institute, 203, B.T. Road, Kolkata 700 108, India

Received 4 December 2006; accepted 31 May 2007
Available online 2 August 2007

Abstract

In a two-layer fluid wherein the upper layer is of finite depth and bounded above by a thin but uniform layer of ice-cover modelled as a thin elastic sheet and the lower layer is infinitely deep below the interface, time-harmonic waves with a given frequency can propagate with two different wavenumbers. The wave of smaller wavenumber propagates along the ice-cover while wave of higher wavenumber propagates along the interface. In this paper problems of wave scattering by a horizontal circular cylinder submerged in either the lower or in the upper layer due to obliquely as well as normally incident wave trains of both the wave numbers are investigated by using the method of multipole expansions. The effect of the presence of ice-cover on the various reflection and transmission coefficients due to incident waves at the ice-cover and the interface is depicted graphically in a number of figures.

Keywords: Two-layer fluid; Wave scattering; Ice-cover; Reflection and transmission coefficients

1. Introduction

Stokes [1] first investigated wave propagation in a two-layer fluid with a free surface and an interface. For such a two-layer fluid it is known that time-harmonic waves with a given frequency can propagate with two different wave numbers (cf. [2]). Linton and McIver [3] developed a general theory for two-dimensional wave propagation in such a two-layer fluid. Due to the presence of an obstacle, an incident wave of a particular wave number gets reflected and transmitted into waves of both the wave numbers, so that on scattering by an obstacle, transfer of energy from one mode to another takes place. When the obstacle is in the form of a horizontal circular cylinder, situated in either the lower or the upper layer, Linton and McIver [3] calculated reflection and transmission coefficients associated with both the wave numbers for a wave train of again both the wave numbers normally incident on the cylinder. They observed that when the cylinder is in the lower layer then the reflection coefficients are identically zero.

This is in conformity with the classical result (cf. [4]) that a horizontal circular cylinder submerged in deep water is transparent to a normally incident wave train. However, the cylinder does experience reflection if it is submerged in the upper layer. This problem arose in connection with modelling an under water pipe bridge across Norwegian fjords consisting of a layer of fresh water on the top of a deep layer of salt water. Linton and Cadby [5] also investigated the problem of scattering of obliquely incident waves by a long circular cylinder in a two-layer fluid and observed that for an incident angle above a critical angle defined by a relation involving the density ratio between the two fluids, there is no transfer of energy from the waves of higher wave number to the waves of lower wave number while for incident angles less than the critical angle, energy transfer only occurs at somewhat higher frequencies, and the phenomenon of zero transmission occurs at some particular frequencies.

There is a considerable interest in the study of various types of water wave problems in the presence of a thin ice-sheet floating on water, termed as water with an ice-cover, the ice-sheet being modelled as a thin elastic plate (cf. [6–13] and others). Das and Mandal [14] investigated the wave scattering by a long circular cylinder in a single-layer fluid of infinite depth with an ice-cover and observed that the cylinder does not experience reflection for normal incidence, but does experience reflection for oblique incidence. This has motivated us to consider a two-layer fluid whose upper layer is bounded above by a thin uniform ice-cover and the lower layer is infinitely deep. In this case, time-harmonic waves of a particular frequency can propagate with two different wave numbers, waves with higher wave number at the interface while waves with lower wave number at the ice-cover.

Wave scattering by a horizontal circular cylinder situated in either of the two layers of an ice-covered two-layer fluid is considered here. A brief account of oblique scattering by a circular cylinder submerged in the lower layer was reported by Das and Mandal [15]. Oblique and normal incidence of a wave train of both the wave numbers are considered here. It is observed that, for normal incidence of a wave train, there is no reflection when the cylinder is in the lower layer. Thus the classical result about the transparency of a circular cylinder due to normally incident surface wave train in an infinitely deep water with a free surface also holds good for a two-layer fluid with an ice-cover if the cylinder is situated in the infinitely deep lower layer. When the circular cylinder is in the upper layer, for normal incidence, there is also no transparency property of the cylinder. Moreover, as observed by Linton and Cadby [5], for a two-layer fluid with a free surface, for oblique incidence, here also there exists a critical angle. For incident angles less than this critical angle, there exist now two cut-off frequencies, and for frequencies lying between these two frequencies will there be a transfer of energy from the waves of higher wave number to the waves of lower wave number in the scattering process. The higher cut-off frequency increases rapidly as the ice-cover parameter decreases, and becomes very large as this parameter becomes very small since the cut-off frequency curve becomes almost asymptotically parallel to the Ka-axis in the (Ka, α)-plane (see Fig. 1), where $K = \sigma^2/g$, σ being the angular frequency, g being the gravity,

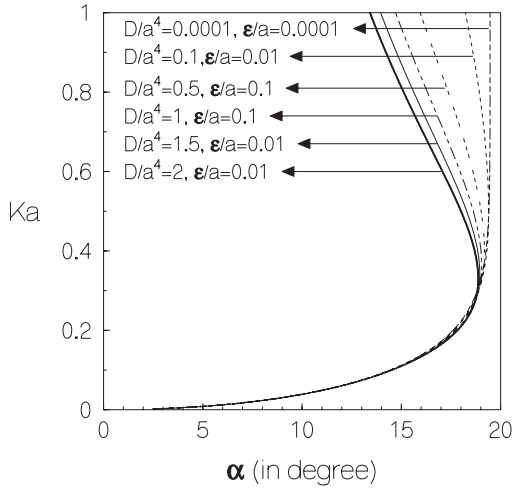

Fig. 1. Cut-off frequency $K_c a$ due to an incident wave of wavenumber λ_2 ($h/a = 2$, $\rho = 0.5$).

a is the radius of the submerged circular cylinder and α is the angle of incidence. In fact the $K_c a$ curve almost coincides with the corresponding $K_c a$ curve for a two-layer fluid with a free surface. For angles less than the critical angle, energy transfer occurs only when the frequency lies between these cut-off frequencies, and when there is no energy transfer, the phenomenon of zero transmission is observed at some particular frequencies.

In Section 2, the general problem of oblique wave incidence in a two-layer fluid with an ice-cover is discussed. The problems of wave scattering (for oblique and normal incidence) by a cylinder are treated in Section 3 when the cylinder is in the lower fluid and in Section 4 when it is in the upper fluid.

Numerical estimates for the reflection and transmission coefficients are obtained and are depicted graphically against the wave number for various values of the angle of incidence and other parameters in a number of figures. For normally incident wave trains, the numerical estimates for reflection and transmission coefficients are also obtained and are depicted graphically against the wave number. The energy identities (derived in Appendix A) are used as a check on the correctness of all numerical results for the reflection and transmission coefficients.

2. Oblique waves scattering in a two-layer fluid

We are here concerned with irrotational motion in two superposed non-viscous incompressible fluids under the action of gravity, neglecting any effect due to surface tension at the interface of the two fluids, the upper being of finite depth h and covered by a thin uniform ice sheet modelled as a thin elastic plate, while the lower layer being infinitely deep. The upper and lower layer fluids have densities ρ_1 and $\rho_2(>\rho_1)$, respectively. Cartesian co-ordinates are chosen such that (x,z)-plane coincides with the undisturbed interface between the two fluids. The y-axis points vertically upwards with $y=0$ as the mean position of the interface and $y=h(>0)$ as the mean position of the thin ice-cover. Under the usual assumptions of linear water wave theory a velocity potential can be defined for oblique waves in the form

$$\Phi(x,y,z,t) = \mathrm{Re}\{\phi(x,y)\mathrm{e}^{-\mathrm{i}\sigma t+\mathrm{i}\gamma z}\},$$

where $\phi(x,y)$ is a complex valued potential function, γ is the wavenumber component along the z-direction and σ is defined earlier.

The upper fluid, $0<y<h$, will be referred to as region I, while the lower fluid, $y<0$, will be referred to as region II. The potential in the upper fluid will be denoted by ϕ^{I} and that in the lower fluid by ϕ^{II}. ϕ^{I} and ϕ^{II} satisfied Helmholtz equation

$$(\nabla^2-\gamma^2)\phi^{\mathrm{I}}=0 \quad \text{for } 0<y<h, \tag{2.1}$$

$$(\nabla^2-\gamma^2)\phi^{\mathrm{II}}=0 \quad \text{for } -\infty<y<0. \tag{2.2}$$

Linearized boundary conditions at the interface and at the ice-cover are

$$\phi^{\mathrm{I}}_y=\phi^{\mathrm{II}}_y \quad \text{on } y=0, \tag{2.3}$$

$$\rho(\phi^{\mathrm{I}}_y-K\phi^{\mathrm{I}})=\phi^{\mathrm{II}}_y-K\phi^{\mathrm{II}} \quad \text{on } y=0, \tag{2.4}$$

where $\rho=\frac{\rho_1}{\rho_2}(<1)$,

$$\left(D\left(\frac{\partial^2}{\partial x^2}-\gamma^2\right)^2+1-\epsilon K\right)\phi^{\mathrm{I}}_y-K\phi^{\mathrm{I}}=0 \quad \text{on } y=h, \tag{2.5}$$

where K is defined earlier, $D=\frac{L}{\rho_1 g}$ where L is the flexural rigidity of the elastic ice-cover and $\epsilon=\frac{\rho_0}{\rho_1}h_0$, ρ_0 is the density of the ice and h_0 is the very small thickness of the ice-cover. The boundary conditions (2.3) and (2.4) are obtained from the continuity of normal velocity and pressure at the interface, respectively.

Also condition at large depth is

$$\nabla\phi^{\mathrm{II}}\to 0 \quad \text{as } y\to-\infty. \tag{2.6}$$

In a two-layer fluid progressive waves have the form (except for a multiplicative constant)

$$\phi^{\mathrm{I}} = \mathrm{e}^{\pm \mathrm{i}x(k^2-\gamma^2)^{\frac{1}{2}}}[\{k(Dk^4+1-\epsilon K)+K\}\mathrm{e}^{k(y-h)} + \{k(Dk^4+1-\epsilon K)-K\}\mathrm{e}^{-k(y-h)}], \tag{2.7}$$

and

$$\phi^{\mathrm{II}} = \mathrm{e}^{\pm \mathrm{i}x(k^2-\gamma^2)^{\frac{1}{2}}}\mathrm{e}^{ky}[\{k(Dk^4+1-\epsilon K)+K\}\mathrm{e}^{-kh} + \{k(Dk^4+1-\epsilon K)-K\}\mathrm{e}^{kh}], \tag{2.8}$$

where k satisfies the dispersion equation

$$\begin{aligned} H(k) \equiv{}& K\rho\{k(Dk^4+1-\epsilon K)\cosh kh - K\sinh kh\} \\ &- \{k(1-\rho)-K\}\{k(Dk^4+1-\epsilon K)\sinh kh - K\cosh kh\} = 0. \end{aligned} \tag{2.9}$$

Eq. (2.9) has exactly two positive real roots λ_1 and $\lambda_2(\lambda_1 < \lambda_2)$ (say). Also, it has one negative real root and four complex roots in the four quadrants of the complex k-plane.

For the case $k = \lambda_j$ $(j = 1,2)$ progressive waves are thus of the form

$$\phi^{\mathrm{I}}(x,y) = \mathrm{e}^{\pm \mathrm{i}\beta_j x} g_j(y), \quad j = 1,2, \tag{2.10}$$

$$\phi^{\mathrm{II}}(x,y) = \mathrm{e}^{\pm \mathrm{i}\beta_j x + \lambda_j y}, \quad j = 1,2, \tag{2.11}$$

where $\beta_j = (\lambda_j^2 - \gamma^2)^{\frac{1}{2}}$ in which that branch of the square root is chosen for which $\beta_j = \lambda_j$ for $\gamma = 0$,

$$\begin{aligned} g_j(y) = {}& \frac{\{\lambda_j(1-\rho)-K\}}{K\rho\{\lambda_j(D\lambda_j^4+1-\epsilon K)\cosh \lambda_j h - K\sinh \lambda_j h\}} \times [\{\lambda_j(D\lambda_j^4+1-\epsilon K)+K\}\mathrm{e}^{\lambda_j(y-h)} \\ &+ \{\lambda_j(D\lambda_j^4+1-\epsilon K)-K\}\mathrm{e}^{-\lambda_j(y-h)}], \quad j = 1,2. \end{aligned} \tag{2.12}$$

We require $\gamma < \lambda_1$ for $j = 1$ and $\gamma < \lambda_2$ for $j = 2$, for the progressive waves to exist.

In any wave scattering problem therefore, the far-field will take the form of incoming and outgoing waves at each of the wave numbers λ_j $(j = 1,2)$. It is given by

$$\phi^{\mathrm{I}} \sim (A^{\pm}\mathrm{e}^{\pm \mathrm{i}\beta_1 x} + C^{\pm}\mathrm{e}^{\mp \mathrm{i}\beta_1 x})g_1(y) + (B^{\pm}\mathrm{e}^{\pm \mathrm{i}\beta_2 x} + D^{\pm}\mathrm{e}^{\mp \mathrm{i}\beta_2 x})g_2(y), \tag{2.13}$$

$$\phi^{\mathrm{II}} \sim (A^{\pm}\mathrm{e}^{\pm \mathrm{i}\beta_1 x} + C^{\pm}\mathrm{e}^{\mp \mathrm{i}\beta_1 x})\mathrm{e}^{\lambda_1 y} + (B^{\pm}\mathrm{e}^{\pm \mathrm{i}\beta_2 x} + D^{\pm}\mathrm{e}^{\mp \mathrm{i}\beta_2 x})\mathrm{e}^{\lambda_2 y}, \tag{2.14}$$

as $x \to \pm\infty$, for which, in the notation of Linton and McIver [3],

$$\phi \sim (A^-, B^-, C^-, D^-; \quad A^+, B^+, C^+, D^+). \tag{2.15}$$

Incident plane wave ϕ_{inc} of wave number λ_1 making an angle $\alpha(0 \leqslant \alpha \leqslant \frac{\pi}{2})$ with the positive x-axis has the form

$$\phi^{\mathrm{I}}_{\mathrm{inc}} = \mathrm{e}^{\mathrm{i}\lambda_1 x\cos\alpha} g_1(y), \tag{2.16}$$

$$\phi^{\mathrm{II}}_{\mathrm{inc}} = \mathrm{e}^{\mathrm{i}\lambda_1 x\cos\alpha + \lambda_1 y}. \tag{2.17}$$

In this case

$$\gamma = \lambda_1 \sin\alpha, \quad \beta_1 = \lambda_1\cos\alpha, \quad \beta_2 = (\lambda_2^2 - \lambda_1^2\sin^2\alpha)^{\frac{1}{2}}. \tag{2.18}$$

It is obvious that β_2 is real since $\lambda_1 < \lambda_2$ and so scattered waves of wave number λ_2 will exist for all values of λ_1 (i.e. for all values of K, since for different values of K, we get different λ_1 and $\lambda_2(>\lambda_1)$) and for all incident angles α. The angle α_{λ_2} for the scattered waves of wave number λ_2 is given by

$$\tan\alpha_{\lambda_2} = \frac{\gamma}{\beta_2} = \frac{\lambda_1\sin\alpha}{(\lambda_2^2 - \lambda_1^2\sin^2\alpha)^{\frac{1}{2}}}. \tag{2.19}$$

Since $\beta_2 > \beta_1$ we know that $\tan\alpha_{\lambda_2} < \tan\alpha$ and hence $\alpha_{\lambda_2} < \alpha$.

An incident plane wave of wave number λ_2 making an angle α $(0 \leqslant \alpha \leqslant \frac{\pi}{2})$ with the positive x-axis is given by

$$\phi^{\mathrm{I}}_{\mathrm{inc}} = \mathrm{e}^{\mathrm{i}\lambda_2 x\cos\alpha} g_2(y), \tag{2.20}$$

$$\phi^{\mathrm{II}}_{\mathrm{inc}} = \mathrm{e}^{\mathrm{i}\lambda_2 x\cos\alpha + \lambda_2 y}. \tag{2.21}$$

In this case

$$\gamma = \lambda_2 \sin\alpha, \quad \beta_1 = (\lambda_1^2 - \lambda_2^2 \sin^2\alpha)^{\frac{1}{2}}, \quad \beta_2 = \lambda_2 \cos\alpha. \tag{2.22}$$

For a given angle α there may be a value of K for which $\lambda_1 = \lambda_2 \sin\alpha$ and thus $\beta_1 = 0$. We will call this K as the *cut-off frequency* and denote it by K_c. For a value of K for which $\lambda_1 > \lambda_2 \sin\alpha$ (for fixed α) we get real β_1 and so waves of wave number λ_1 will propagate. For a value of K for which $\lambda_1 < \lambda_2 \sin\alpha$ (for fixed α) β_1 becomes imaginary and in that case there exists no propagating wave of wave number λ_1. Fig. 1 shows the cut-off frequency $K_c a$, plotted against incident wave angle

$$\alpha = \sin^{-1}\left(\frac{\lambda_1}{\lambda_2}\right), \tag{2.23}$$

for density ratio $\rho = 0.5$, $h/a = 2$, and different values of $\frac{D}{a^4}$ and ϵ/a, a being the radius of the circular cylinder considered in the next section. Instead of using a, we could have used h to non-dimensionalise ϵ and D, but that would not have changed this discussion.

The different curves in Fig. 1 correspond to $\frac{D}{a^4} = 2, 1.5, 1, 0.5, 0.1$ and $\epsilon/a = 0.01$ (except one curve for which $\epsilon/a = 0.0001$, $\frac{D}{a^4} = 0.0001$). It is observed from this figure that for any angle α for which the point (α, Ka) is situated on the right side of the curve there are no propagating waves of wave number λ_1 for this value of Ka. It may be noted that for very small value of $\frac{D}{a^4}$ i.e. 0.0001 with small $\epsilon/a = 0.0001$, the curve almost coincides with the curve for the case of upper fluid with a free surface (Fig. 1 in [6]). Due to the presence of ice-cover, we observe from this figure that for some values of α for which the point (Ka, α) is situated on the left side of the curve there are two cut-off frequencies and only for frequencies lying between these two cut-off frequencies will there be conversion of wave number λ_1 from wave of wave number λ_2. In Fig. 2, the critical angle α_c is plotted against $\frac{D}{a^4}$, for $K_c a = 0.3, 0.5, 0.9$. These curves show that α_c decreases as $\frac{D}{a^4}$ increases for higher values of $K_c a$.

When waves of wave number λ_1 propagates, the angle α_{λ_1} of the scattered waves of wave number λ_1 is given by

$$\tan\alpha_{\lambda_1} = \frac{\lambda_2 \sin\alpha}{(\lambda_1^2 - \lambda_2^2 \sin^2\alpha)^{\frac{1}{2}}}. \tag{2.24}$$

In the case of a single-layer fluid, for any scattering problem, the reflection and transmission coefficients satisfy the energy identity, which is generally used as a partial check on the correctness of the analytical or computed values of these coefficients. For a two-layer fluid with a free surface, there exists two energy identities corresponding to scattering of incident waves of two different wave numbers (cf. [3,6]). These energy identities were

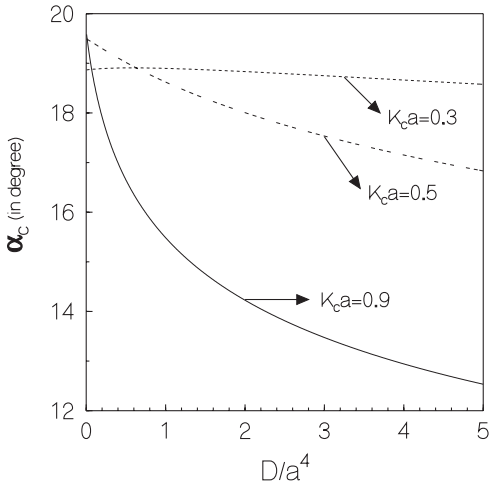

Fig. 2. Critical angle α_c for a fixed cut-off frequency ($\varepsilon/a = 0.01$, $h/a = 2$, $\rho = 0.5$).

derived by appropriate uses of Green's integral theorem. For a two-layer fluid in which the upper layer has an ice-cover instead of a free surface, energy identities are derived here in Appendix A by using a generalized form of Green's integral theorem. These identities are used here as partial numerical checks for all the data points in obtaining the various curves for the reflection and transmission coefficients.

3. Cylinder in the lower layer

Let a horizontal circular cylinder of radius a have its axis at $y = f(<0)$ and its generator runs parallel to z-axis. Polar co-ordinates (r,θ) are defined in the (x,y)-plane by

$$x = r\sin\theta \quad \text{and} \quad y = f - r\cos\theta. \tag{3.1}$$

Let the symmetric and antisymmetric multipoles be defined by $\phi_n^{\mathrm{s}}(n \geqslant 0)$ and $\phi_n^{\mathrm{a}}(n \geqslant 1)$, respectively. The multipoles are defined by (in the notation of Linton and Cadby [6])

$$\phi_n^{\mathrm{Is}} = (-1)^n \int_0^\infty \cosh nk \cos(\gamma x \sinh k)(A(k)\mathrm{e}^{vy} + B(k)\mathrm{e}^{-vy})\,\mathrm{d}k, \tag{3.2}$$

$$\phi_n^{\mathrm{IIs}} = K_n(\gamma r)\cos n\theta + (-1)^n \int_0^\infty \cosh nk \cos(\gamma x \sinh k)C(k)\mathrm{e}^{vy}\,\mathrm{d}k, \tag{3.3}$$

$$\phi_n^{\mathrm{Ia}} = (-1)^{n+1} \int_0^\infty \sinh nk \sin(\gamma x \sinh k)(A(k)\mathrm{e}^{vy} + B(k)\mathrm{e}^{-vy})\,\mathrm{d}k, \tag{3.4}$$

$$\phi_n^{\mathrm{IIa}} = K_n(\gamma r)\sin n\theta + (-1)^{n+1} \int_0^\infty \sinh nk \sin(\gamma x \sinh k)C(k)\mathrm{e}^{vy}\,\mathrm{d}k, \tag{3.5}$$

where $v = \gamma\cosh k$ and $A(k)$, $B(k)$, $C(k)$ are functions of k to be found such that the integrals exist in some sense. $K_n(z)$ is the modified Bessel function of second kind.

The functions ϕ_n^{s} and ϕ_n^{a} are singular solutions of the modified Helmholtz equation and satisfy the ice-cover condition (2.5) and the interface conditions (2.3) and (2.4) and are of outgoing nature at infinity. Then $A(k)$, $B(k)$ and $C(k)$ have the forms

$$A(k) = K\{v(Dv^4 + 1 - \epsilon K) + K\}\mathrm{e}^{v(f-h)}/H(v), \tag{3.6}$$

$$B(k) = K\{v(Dv^4 + 1 - \epsilon K) - K\}\mathrm{e}^{v(f+h)}/H(v), \tag{3.7}$$

$$\begin{aligned} C(k) = {} & [K\rho\{v(Dv^4 + 1 - \epsilon K)\cosh vh - K\sinh vh\} \\ & - \{(1-\rho)v + K\}\{v(Dv^4 + 1 - \epsilon K)\sinh vh - K\cosh vh\}]\mathrm{e}^{vf}/H(v), \end{aligned} \tag{3.8}$$

where $H(v)$ is given by (2.9) (with k replaced by v).

The path of the integration in the integrals in (3.2)–(3.5) is indented below the poles at $k = \mu_1$ and $k = \mu_2$, where

$$\gamma\cosh\mu_j = \lambda_j, \quad j = 1,2. \tag{3.9}$$

The far-field forms of the multipoles, in the lower fluid, are given by

$$\phi_n^{\mathrm{IIs}} \sim (-1)^n \pi\mathrm{i}(C^{\mu_1}\cosh n\mu_1 \mathrm{e}^{\pm\mathrm{i}\beta_1 x + \lambda_1 y} + C^{\mu_2}\cosh n\mu_2 \mathrm{e}^{\pm\mathrm{i}\beta_2 x + \lambda_2 y}), \tag{3.10}$$

$$\phi_n^{\mathrm{IIa}} \sim \mp(-1)^n \pi(C^{\mu_1}\sinh n\mu_1 \mathrm{e}^{\pm\mathrm{i}\beta_1 x + \lambda_1 y} + C^{\mu_2}\sinh n\mu_2 \mathrm{e}^{\pm\mathrm{i}\beta_2 x + \lambda_2 y}), \tag{3.11}$$

as $x \to \pm\infty$, where C^{μ_1} and C^{μ_2} are the residues of $C(k)$ at $k = \mu_1$ and $k = \mu_2$, and these are given by

$$\begin{aligned} C^{\mu_j} = {} & [K\rho\{\lambda_j(D\lambda_j^4 + 1 - \epsilon K)\cosh\lambda_j h - K\sinh\lambda_j h\} \\ & - \{(1-\rho)\lambda_j + K\}\{\lambda_j(D\lambda_j^4 + 1 - \epsilon K)\sinh\lambda_j h - K\cosh\lambda_j h\}]\mathrm{e}^{\lambda_j f}/\beta_j H'(\lambda_j), \quad j = 1,2. \end{aligned} \tag{3.12}$$

Using the expansion

$$\mathrm{e}^{\frac{1}{2}X(P+P^{-1})} = \sum_{m=0}^{\infty} \frac{1}{2}\epsilon_m (P^m + P^{-m}) I_m(X), \tag{3.13}$$

where

$$\epsilon_0 = 1, \quad \epsilon_m = 2, \quad m \geqslant 1. \tag{3.14}$$

$I_m(X)$ is the modified Bessel function of first kind, (3.3) and (3.5) can be expanded in terms of polar co-ordinates as

$$\phi_n^{\mathrm{IIs}} = K_n(\gamma r)\cos n\theta + \sum_{m=0}^{\infty} A_{nm}^{(s)} I_m(\gamma r)\cos m\theta, \tag{3.15}$$

$$\phi_n^{\mathrm{IIa}} = K_n(\gamma r)\sin n\theta + \sum_{m=1}^{\infty} A_{nm}^{(a)} I_m(\gamma r)\sin m\theta, \tag{3.16}$$

where

$$A_{nm}^{(s)} = \epsilon_m(-1)^{m+n}\int_0^{\infty} \mathrm{e}^{vf}\cosh mk\cosh nkC(k)\,\mathrm{d}k, \tag{3.17}$$

$$A_{nm}^{(a)} = 2(-1)^{m+n}\int_0^{\infty} \mathrm{e}^{vf}\sinh mk\sinh nkC(k)\,\mathrm{d}k. \tag{3.18}$$

3.1. Obliquely incident wave train of wavenumber λ_1

Let us consider the case of an obliquely wave train of wavenumber λ_1 making an angle α with the positive x-axis, so that $\gamma = \lambda_1\sin\alpha$. The incident wave potential (2.17) has the form

$$\phi_{\mathrm{inc}}^{\mathrm{II}} = \mathrm{e}^{\mathrm{i}\beta_1 x + \lambda_1 y} = \mathrm{e}^{\lambda_1 f}\sum_{m=0}^{\infty}\epsilon_m(-1)^m I_m(\gamma r)(\cosh mv\cos m\theta - \mathrm{i}\sinh mv\sin m\theta), \tag{3.19}$$

where

$$\cosh v = \frac{\lambda_1}{\gamma} = \frac{1}{\sin\alpha}.$$

To solve the scattering problem we write the potential function describing the fluid motion as

$$\phi_{\lambda_1} = \phi_{\mathrm{inc}} + \sum_{n=0}^{\infty}(a_n\phi_n^{\mathrm{a}} + b_n\phi_n^{\mathrm{s}}), \tag{3.20}$$

where a_n and b_n are unknown constants to be determined.

To find a_n and b_n the polar expansions of the multipoles (3.3), (3.5) and the incident wave (3.19) are substituted into (3.20). Applying the body boundary condition $\frac{\partial\phi_{\lambda_1}^{\mathrm{II}}}{\partial r} = 0$ on $r = a$, and using the orthogonal properties of the trigonometric functions, we obtain two infinite systems of linear equations for the unknowns a_n and b_n as given by,

$$\frac{a_m}{Z_m} + \sum_{n=1}^{\infty} A_{nm}^{(a)} a_n = 2\mathrm{i}(-1)^m \mathrm{e}^{\lambda_1 f}\sinh mv, \quad m = 1, 2, \ldots, \tag{3.21}$$

$$\frac{b_m}{Z_m} + \sum_{n=0}^{\infty} A_{nm}^{(s)} b_n = (-1)^{m+1}\epsilon_m \mathrm{e}^{\lambda_1 f}\cosh mv, \quad m = 0, 1, \ldots, \tag{3.22}$$

where

$$Z_m = \frac{I_m'(\gamma a)}{K_m'(\gamma a)},$$

dash denoting derivative with respect to the arguments.

These two systems can be solved by truncation. Here 5×5 systems were used as in [6] for numerical computations.

The far-field form for $\phi^{\mathrm{II}}_{\lambda_1}$, in the lower layer, can be written as

$$\phi^{\mathrm{II}}_{\lambda_1} \sim \begin{cases} \mathrm{e}^{\mathrm{i}\beta_1 x+\lambda_1 y} + R_{\lambda_1}\mathrm{e}^{-\mathrm{i}\beta_1 x+\lambda_1 y} + r_{\lambda_1}\mathrm{e}^{-\mathrm{i}\beta_2 x+\lambda_2 y} & \text{as } x \to -\infty, \\ T_{\lambda_1}\mathrm{e}^{\mathrm{i}\beta_1 x+\lambda_1 y} + t_{\lambda_1}\mathrm{e}^{\mathrm{i}\beta_2 x+\lambda_2 y} & \text{as } x \to \infty. \end{cases} \tag{3.23}$$

Using (3.20), (3.10) and (3.11) we obtain the reflection and transmission coefficients as follows:

$$R_{\lambda_1} = \pi C^{\mu_1} \sum_{m=0}^{\infty} (-1)^m \{\mathrm{i}b_m \cosh m\mu_1 + a_m \sinh m\mu_1\}, \tag{3.24}$$

$$r_{\lambda_1} = \pi C^{\mu_2} \sum_{m=0}^{\infty} (-1)^m \{\mathrm{i}b_m \cosh m\mu_2 + a_m \sinh m\mu_2\}, \tag{3.25}$$

$$T_{\lambda_1} = 1 + \pi C^{\mu_1} \sum_{m=0}^{\infty} (-1)^m \{\mathrm{i}b_m \cosh m\mu_1 - a_m \sinh m\mu_1\}, \tag{3.26}$$

$$t_{\lambda_1} = \pi C^{\mu_2} \sum_{m=0}^{\infty} (-1)^m \{\mathrm{i}b_m \cosh m\mu_2 - a_m \sinh m\mu_2\}. \tag{3.27}$$

3.2. Obliquely incident wave train of wavenumber λ_2

We consider the case of an obliquely incident plane wave of wavenumber λ_2 making an angle α with the positive x-axis, so that $\gamma = \lambda_2 \sin\alpha$. The expansion of incident wave potential is the same as (3.19), except that λ_1 is to be replaced by λ_2. The velocity potential ϕ_{λ_2} for this problem can again be expanded in terms of multipoles similar to (3.20) and the equations for a_n and b_n are similar to (3.21) and (3.22) with λ_1 is to be replaced by λ_2.

The far-field forms of $\phi^{\mathrm{II}}_{\lambda_2}$, in the lower layer, can be written as

$$\phi^{\mathrm{II}}_{\lambda_2} \sim \begin{cases} \mathrm{e}^{\mathrm{i}\beta_2 x+\lambda_2 y} + R_{\lambda_2}\mathrm{e}^{-\mathrm{i}\beta_1 x+\lambda_1 y} + r_{\lambda_2}\mathrm{e}^{-\mathrm{i}\beta_2 x+\lambda_2 y} & \text{as } x \to -\infty, \\ T_{\lambda_2}\mathrm{e}^{\mathrm{i}\beta_1 x+\lambda_1 y} + t_{\lambda_2}\mathrm{e}^{\mathrm{i}\beta_2 x+\lambda_2 y} & \text{as } x \to \infty. \end{cases} \tag{3.28}$$

Using the far-field forms of the multipoles given by (3.10) and (3.11) in ϕ_{λ_2} we find that the expressions for reflection coefficients R_{λ_2} and r_{λ_2} are similar to (3.24) and (3.25) with appropriate changes, and the transmission coefficients are given by

$$T_{\lambda_2} = \pi C^{\mu_1} \sum_{m=0}^{\infty} (-1)^m \{\mathrm{i}b_m \cosh m\mu_1 - a_m \sinh m\mu_1\}, \tag{3.29}$$

$$t_{\lambda_2} = 1 + \pi C^{\mu_2} \sum_{m=0}^{\infty} (-1)^m \{\mathrm{i}b_m \cosh m\mu_2 - a_m \sinh m\mu_2\}. \tag{3.30}$$

3.3. Normally incident wave train

Now for the case of normal incidence, $\alpha = 0$, the modified Helmholtz equation reduces to the Laplace's equation and solutions of Laplace's equation singular at $y = f < 0$ are $r^{-n}\cos n\theta$ and $r^{-n}\sin n\theta$, $n \geqslant 1$, and these have the integral representations

$$\frac{\cos n\theta}{r^n} = \frac{(-1)^n}{(n-1)!} \int_0^{\infty} k^{n-1}\mathrm{e}^{-k(y-f)} \cos kx \, \mathrm{d}k,$$

$$\frac{\sin n\theta}{r^n} = \frac{(-1)^{n+1}}{(n-1)!} \int_0^{\infty} k^{n-1}\mathrm{e}^{-k(y-f)} \sin kx \, \mathrm{d}k.$$

It is straightforward to add suitable solutions of Laplace's equation to the symmetric and antisymmetric multipoles so that the boundary conditions are satisfied. We obtain

$$\phi_n^{\mathrm{Is}} = \frac{(-1)^n}{(n-1)!}\int_0^\infty k^{n-1}(A(k)\mathrm{e}^{ky} + B(k)\mathrm{e}^{-ky})\cos kx\,\mathrm{d}k, \tag{3.31}$$

$$\phi_n^{\mathrm{IIs}} = \frac{\cos n\theta}{r^n} + \frac{(-1)^n}{(n-1)!}\int_0^\infty k^{n-1}C(k)\mathrm{e}^{ky}\cos kx\,\mathrm{d}k, \tag{3.32}$$

$$\phi_n^{\mathrm{Ia}} = \frac{(-1)^{n+1}}{(n-1)!}\int_0^\infty k^{n-1}(A(k)\mathrm{e}^{ky} + B(k)\mathrm{e}^{-ky})\sin kx\,\mathrm{d}k, \tag{3.33}$$

$$\phi_n^{\mathrm{IIa}} = \frac{\sin n\theta}{r^n} + \frac{(-1)^{n+1}}{(n-1)!}\int_0^\infty k^{n-1}C(k)\mathrm{e}^{ky}\sin kx\,\mathrm{d}k, \tag{3.34}$$

where now

$$A(k) = K\{k(Dk^4 + 1 - \epsilon K) + K\}\mathrm{e}^{k(f-h)}/H(k), \tag{3.35}$$

$$B(k) = K\{k(Dk^4 + 1 - \epsilon K) - K\}\mathrm{e}^{k(f+h)}/H(k), \tag{3.36}$$

$$\begin{aligned} C(k) = {} & [K\rho\{k(Dk^4 + 1 - \epsilon K)\cosh kh - K\sinh kh\} \\ & - \{(1-\rho)k + K\}\{k(Dk^4 + 1 - \epsilon K)\sinh kh - K\cosh kh\}]\mathrm{e}^{kf}/H(k) \end{aligned} \tag{3.37}$$

and the path of integration is indented to pass beneath the poles of the above four integrands at $k = \lambda_1$ and $k = \lambda_2$. Here we have used the same notation without any confusion.

The multipoles (3.32) and (3.34) can be expanded about $r = 0$. Thus we obtain

$$\phi_n^{\mathrm{IIs}} = \frac{\cos n\theta}{r^n} + \sum_{m=0}^\infty A_{nm} r^m \cos m\theta, \tag{3.38}$$

$$\phi_n^{\mathrm{IIa}} = \frac{\sin n\theta}{r^n} + \sum_{m=0}^\infty A_{nm} r^m \sin m\theta, \tag{3.39}$$

where

$$A_{nm} = \frac{(-1)^{n+m}}{(n-1)!m!}\int_0^\infty k^{n+m-1}C(k)\mathrm{e}^{ky}\,\mathrm{d}k. \tag{3.40}$$

Note that A_{nm} is the same for ϕ_n^{IIs} and ϕ_n^{IIa}.

The far-field form of the multipoles, in the lower layer, is given by

$$\phi_n^{\mathrm{IIs}} \sim \frac{(-1)^n}{(n-1)!}\pi i(\lambda_1^{n-1}C^{\lambda_1}\mathrm{e}^{\pm \mathrm{i}\lambda_1 x + \lambda_1 y} + \lambda_2^{n-1}C^{\lambda_2}\mathrm{e}^{\pm \mathrm{i}\lambda_2 x + \lambda_2 y}), \tag{3.41}$$

$$\phi_n^{\mathrm{IIa}} \sim \mp\frac{(-1)^n}{(n-1)!}\pi(\lambda_1^{n-1}C^{\lambda_1}\mathrm{e}^{\pm \mathrm{i}\lambda_1 x + \lambda_1 y} + \lambda_2^{n-1}C^{\lambda_2}\mathrm{e}^{\pm \mathrm{i}\lambda_2 x + \lambda_2 y}), \tag{3.42}$$

as $x \to \pm\infty$. Here C^{λ_1} C^{λ_2} are the residues of $C(k)$ at $k = \lambda_1$ and $k = \lambda_2$, given by

$$\begin{aligned} C^{\lambda_j} = {} & [K\rho\{\lambda_j(D\lambda_j^4 + 1 - \epsilon K)\cosh \lambda_j h - K\sinh \lambda_j h\} \\ & - \{(1-\rho)\lambda_j + K\}\{\lambda_j(D\lambda_j^4 + 1 - \epsilon K)\sinh \lambda_j h - K\cosh \lambda_j h\}]\mathrm{e}^{\lambda_j f}/H'(\lambda_j), \quad j = 1, 2. \end{aligned} \tag{3.43}$$

3.4. Normally incident wave train of wavenumber λ_1

The incident wave potential

$$\phi_{\mathrm{inc}}^{\mathrm{II}} = \mathrm{e}^{\mathrm{i}\lambda_1 x + \lambda_1 y}, \tag{3.44}$$

when expanded about $r = 0$, has the form

$$\phi_{\mathrm{inc}}^{\mathrm{II}} = \sum_{m=0}^\infty \frac{(-1)^m}{m!}\lambda_1^m r^m(\cos m\theta - \mathrm{i}\sin m\theta)\mathrm{e}^{\lambda_1 f}. \tag{3.45}$$

To solve this scattering problem we write

$$\phi^{\mathrm{II}}_{\lambda_1} = \phi^{\mathrm{II}}_{\mathrm{inc}} + \sum_{n=1}^{\infty} a^n (a_n \phi^{\mathrm{a}}_n + b_n \phi^{\mathrm{s}}_n), \tag{3.46}$$

where a_n and b_n are unknown constants to be determined.

To solve for a_n and b_n the polar expansions of the multipoles (3.32), (3.34) and the incident wave (3.45) are substituted into (3.46) and applying the body boundary condition $\frac{\partial \phi^{\mathrm{II}}_{\lambda_1}}{\partial r} = 0$ on $r = a$ and using the orthogonal properties of the trigonometric functions, we obtain two infinite systems of linear equations for unknowns a_n and b_n which are

$$a_m - \sum_{n=1}^{\infty} a^{n+m} A_{nm} a_n = -\mathrm{i} \frac{(-\lambda_1 a)^m}{m!} \mathrm{e}^{\lambda_1 f}, \quad m = 1, 2, \ldots, \tag{3.47}$$

$$b_m - \sum_{n=1}^{\infty} a^{n+m} A_{nm} b_n = \frac{(-\lambda_1 a)^m}{m!} \mathrm{e}^{\lambda_1 f}, \quad m = 1, 2, \ldots. \tag{3.48}$$

Since left-hand sides of the systems of equations are of the same nature and the right-hand sides of the systems differ by a factor $-\mathrm{i}$, we find that

$$a_n = -\mathrm{i} b_n. \tag{3.49}$$

Thus $\phi^{\mathrm{II}}_{\lambda_1}$ is obtained as

$$\phi^{\mathrm{II}}_{\lambda_1} = \phi^{\mathrm{II}}_{\mathrm{inc}} + \sum_{n=1}^{\infty} a^n b_n (\phi^{\mathrm{s}}_n - \mathrm{i}\phi^{\mathrm{a}}_n), \tag{3.50}$$

It follows immediately from (3.41) and (3.42) that as $x \to -\infty$

$$\phi^{\mathrm{II}}_{\lambda_1} \sim \phi^{\mathrm{II}}_{\mathrm{inc}}. \tag{3.51}$$

The far-field form for $\phi^{\mathrm{II}}_{\lambda_1}$ in the lower fluid can be written as

$$\phi^{\mathrm{II}}_{\lambda_1} \sim \begin{cases} \mathrm{e}^{\mathrm{i}\lambda_1 x + \lambda_1 y} + R_{\lambda_1} \mathrm{e}^{-\mathrm{i}\lambda_1 x + \lambda_1 y} + r_{\lambda_1} \mathrm{e}^{-\mathrm{i}\lambda_2 x + \lambda_2 y} & \text{as } x \to -\infty, \\ T_{\lambda_1} \mathrm{e}^{\mathrm{i}\lambda_1 x + \lambda_1 y} + t_{\lambda_1} \mathrm{e}^{\mathrm{i}\lambda_2 x + \lambda_2 y} & \text{as } x \to \infty. \end{cases} \tag{3.52}$$

Using (3.50) we can obtain the reflection and transmission coefficients:

$$R_{\lambda_1} = r_{\lambda_1} \equiv 0, \tag{3.53}$$

$$T_{\lambda_1} = 1 + 2\pi\mathrm{i} \sum_{n=1}^{\infty} \frac{(-1)^n}{(n-1)!} a^n \lambda_1^{n-1} C^{\lambda_1} b_n, \tag{3.54}$$

$$t_{\lambda_1} = 2\pi\mathrm{i} \sum_{n=1}^{\infty} \frac{(-1)^n}{(n-1)!} a^n \lambda_2^{n-1} C^{\lambda_2} b_n. \tag{3.55}$$

3.5. Normally incident wave train of wavenumber λ_2

For an incident wave of wave number λ_2 the mathematical analysis is the same except that λ_1 is to be replaced by λ_2 in the above equations. Also the far-field forms of $\phi^{\mathrm{II}}_{\lambda_2}$, in the lower layer, can be written as

$$\phi^{\mathrm{II}}_{\lambda_2} \sim \begin{cases} \mathrm{e}^{\mathrm{i}\lambda_2 x + \lambda_2 y} + R_{\lambda_2} \mathrm{e}^{-\mathrm{i}\lambda_1 x + \lambda_1 y} + r_{\lambda_2} \mathrm{e}^{-\mathrm{i}\lambda_2 x + \lambda_2 y} & \text{as } x \to -\infty, \\ T_{\lambda_2} \mathrm{e}^{\mathrm{i}\lambda_1 x + \lambda_1 y} + t_{\lambda_2} \mathrm{e}^{\mathrm{i}\lambda_2 x + \lambda_2 y} & \text{as } x \to \infty. \end{cases} \tag{3.56}$$

Here also we find that the reflection coefficients R_{λ_2} and r_{λ_2} are identically zero. For the transmission coefficients we obtain

$$T_{\lambda_2} = 2\pi i \sum_{n=1}^{\infty} \frac{(-1)^n}{(n-1)!} a^n \lambda_1^{n-1} C^{\lambda_1} b_n, \tag{3.57}$$

$$t_{\lambda_2} = 1 + 2\pi i \sum_{n=1}^{\infty} \frac{(-1)^n}{(n-1)!} a^n \lambda_2^{n-1} C^{\lambda_2} b_n. \tag{3.58}$$

3.6. Numerical results

In Figs. 3–6 the reflection and transmission coefficients are shown for the case of a wave train of wave number λ_1 obliquely incident on the cylinder submerged in the lower fluid. In all the plots immersion depth $-f/a$ is 2, the depth of the upper fluid layer h/a is 2 and ρ (density ratio) is 0.5, $\epsilon/a = 0.01$ and $D/a^4 = 1.5$. The different curves correspond to different incident wave angle α, which are 15°, 75°, 80°, 85°, 89°. From Figs. 3 and 5 it is observed that as the angle of incidence increases, $|R_{\lambda_1}|$ increases while $|T_{\lambda_1}|$ decreases. Also $|R_{\lambda_1}|$

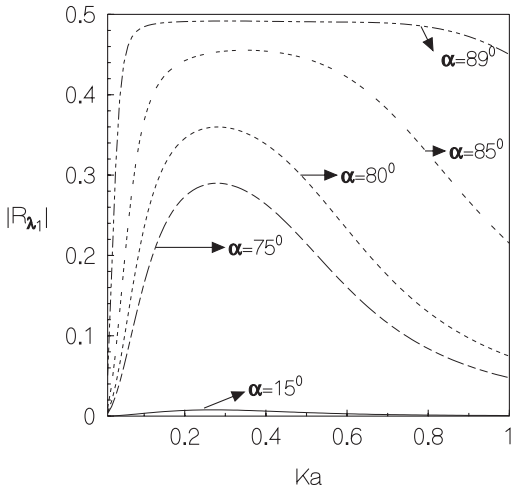

Fig. 3. Reflection coefficient due to a wave of wavenumber λ_1 incident on a cylinder in the lower layer ($D/a^4 = 1.5$, $\varepsilon = .01$, $h/a = 2$, $\rho = .5$, $f/a = -2$).

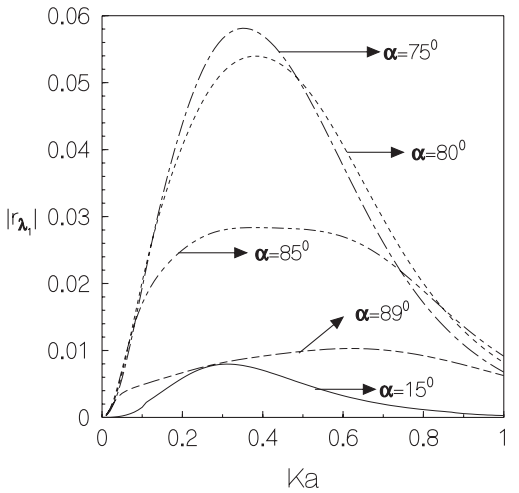

Fig. 4. Reflection coefficient due to a wave of wavenumber λ_1 incident on a cylinder in the lower layer ($D/a^4 = 1.5$, $\varepsilon/a = 0.01$, $\rho = .5$, $h/a = 2$, $f/a = -2$).

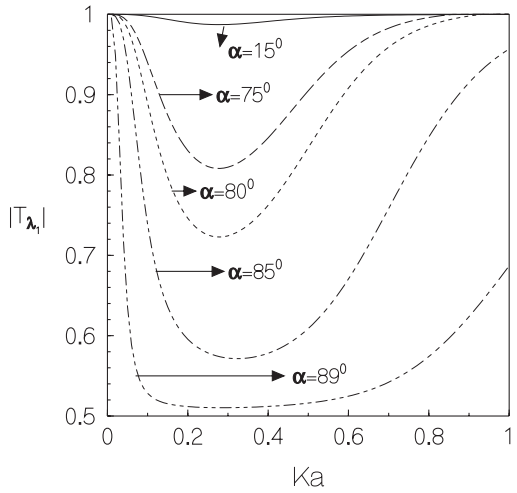

Fig. 5. Transmission coefficient due to a wave of wavenumber λ_1 incident on a cylinder in the lower layer ($D/a^4 = 1.5$, $\varepsilon/a = 0.01$, $h/a = 2$, $\rho = .5$, $f/a = -2$).

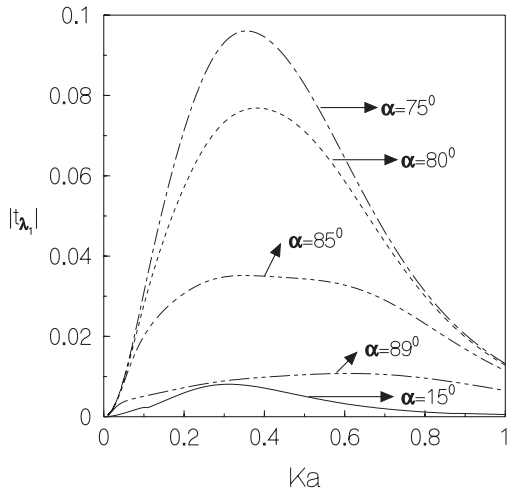

Fig. 6. Transmission coefficient due to a wave of wavenumber λ_1 incident on a cylinder in the lower layer ($D/a^4 = 1.5$, $\varepsilon/a = 0.01$, $\rho = .5$, $h/a = 2$, $f/a = -2$).

is somewhat smaller in comparison to that of Linton and Cadby [6] and $|T_{\lambda_1}|$ is somewhat larger in comparison to that of Linton and Cadby [6]. This is due to the presence of the ice-cover. For $\alpha = 15°$, the reflection coefficient $|R_{\lambda_1}|$ is seen to be quite small. In fact for small α, $|R_{\lambda_1}|$ becomes negligible.

The reflection coefficient $|r_{\lambda_1}|$ and transmission coefficient $|t_{\lambda_1}|$ of waves of wave number λ_2 for an incident wave of wave number λ_1, shown in Figs. 4 and 6, respectively, are smaller in comparison to those for wave of wave number λ_1, but their non-zero values show that there is some conversion of energy from one wave number to the other.

The case of an incident wave of wave number λ_2 is more interesting due to the presence of cut-off frequencies. For this case, Figs. 7–10 show the reflection coefficients $|R_{\lambda_2}|$, $|r_{\lambda_2}|$ and transmission coefficients $|T_{\lambda_2}|$, $|t_{\lambda_2}|$ against Ka for $h/a = 2$, $\rho = 0.5$, $f/2 = -2$, $\epsilon/a = 0.01$, $D/a^4 = 1.5$. The different curves correspond to different values of the incident angle α, viz. 14.9°, 16.6°, 17.76°, 19.20°. When $\alpha = 19.20°$ which is greater than the critical angle $\alpha_c = 18.95°$ for the given values of the different parameters, there is no wave of wave number λ_1 propagating in the fluid. From Fig. 1 we have the following cut-off frequencies: $K_c a = (0.09, 0.86)$; $(0.13, 0.665)$; $(0.17, 0.54)$ corresponding to the incident angles 14.9°, 16.6°, 17.76°, respectively. For these

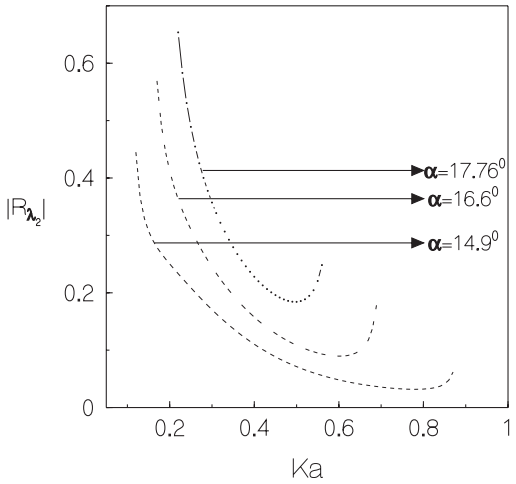

Fig. 7. Reflection coefficient due to a wave of wavenumber λ_2 incident on a cylinder in the lower layer ($D/a^4 = 1.5$, $\varepsilon/a = 0.01$, $h/a = 2$, $\rho = 0.5$, $f/a = -2$).

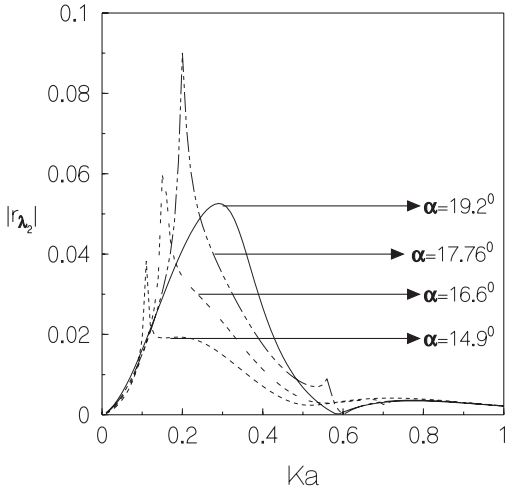

Fig. 8. Reflection coefficient due to a wave of wavenumber λ_2 incident on a cylinder in the lower layer ($D/a^4 = 1.5$, $\varepsilon/a = 0.01$, $h/a = 2$, $\rho = 0.5$, $f/a = -2$).

angles and for frequencies lying between two appropriate cut-off frequencies will there be conversion of energy from one mode to the other. $|r_{\lambda_2}|$, $|t_{\lambda_2}|$ for the incident wave number λ_2 are shown in Figs. 8 and 10. From these two figures we observe that for a particular frequency just less than the cut-off frequency there is maximum reflection and minimum transmission of the incident wave of wave number λ_2. For $\alpha = 14.9°$, $16.6°$, $17.76°$ there are two spikes in the curves because of two cut-off frequencies. When $\alpha = 19.20°$ which is greater than the critical angle, there is no spike on the curve. All the numerical values of the reflection and transmission coefficients have been checked for their correctness from the energy identities.

For the case of normal incidence, Figs. 11 and 12 show the transmission coefficients for the case of an incident wave of wave number λ_1 incident on a circular cylinder in the lower fluid for $\epsilon/a = 0.01$, $h/a = 2$, $\rho = 0.5$, $f/a = -2$. The different curves correspond to different values of D/a^4, $D/a^4 = 0.1, 0.5, 1,\ 1.5, 2$. Fig. 11 shows that $|T_{\lambda_1}|$ first decreases as Ka increases for low to moderate values of Ka but it increases as Ka further increases for any D/a^4. Fig. 12 describes the behavior of $|t_{\lambda_1}|$ which is complimentary to the behavior of $|T_{\lambda_1}|$. Also Figs. 13 and 14 show the transmission coefficients due to a wave of wave number λ_2 incident on a cylinder in the lower layer. Fig. 13 (Fig. 14) describes the behavior of $|T_{\lambda_2}|$ which is similar to the behavior of $|t_{\lambda_2}|(|T_{\lambda_2}|)$.

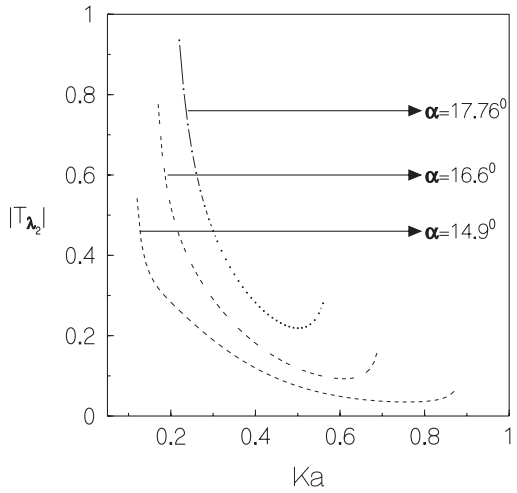

Fig. 9. Transmission coefficient due to a wave of wavenumber λ_2 incident on a cylinder in the lower layer ($D/a^4 = 1.5$, $\varepsilon/a = 0.01$, $\rho = 0.5$, $h/a = 2$, $f/a = -2$).

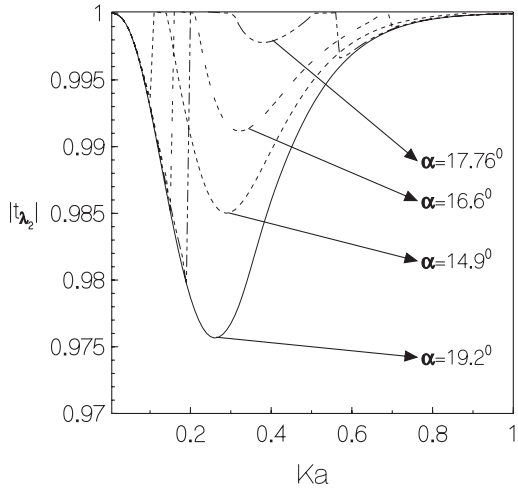

Fig. 10. Transmission coefficient due to a wave of wavenumber λ_2 incident on a cylinder in the lower layer ($D/a^4 = 1.5$, $\varepsilon/a = 0.01$, $h/a = 2$, $\rho = 0.5$, $f/a = -2$).

4. Cylinder in the upper layer

A horizontal circular cylinder of radius a has its axis at $y = f(>0)$ and its generator runs parallel to the z-axis ($f/a > 1$). Polar co-ordinates are again defined via (3.1) and suitable multipoles have the forms

$$\phi_n^{\mathrm{Is}} = K_n(\gamma r)\cos n\theta + \int_0^\infty \cosh nk \cos(\gamma x \sinh k)(A_n^{(0)}(k)\mathrm{e}^{vy} + B_n^{(0)}(k)\mathrm{e}^{-vy})\,\mathrm{d}k, \tag{4.1}$$

$$\phi_n^{\mathrm{IIs}} = \int_0^\infty \cosh nk \cos(\gamma x \sinh k) C_n^{(0)}(k)\mathrm{e}^{vy}\,\mathrm{d}k, \tag{4.2}$$

$$\phi_n^{\mathrm{Ia}} = K_n(\gamma r)\sin n\theta + \int_0^\infty \sinh nk \sin(\gamma x \sinh k)(A_n^{(1)}(k)\mathrm{e}^{vy} + B_n^{(1)}(k)\mathrm{e}^{-vy})\,\mathrm{d}k, \tag{4.3}$$

$$\phi_n^{\mathrm{IIa}} = \int_0^\infty \sinh nk \sin(\gamma x \sinh k) C_n^{(1)}(k)\mathrm{e}^{vy}\,\mathrm{d}k, \tag{4.4}$$

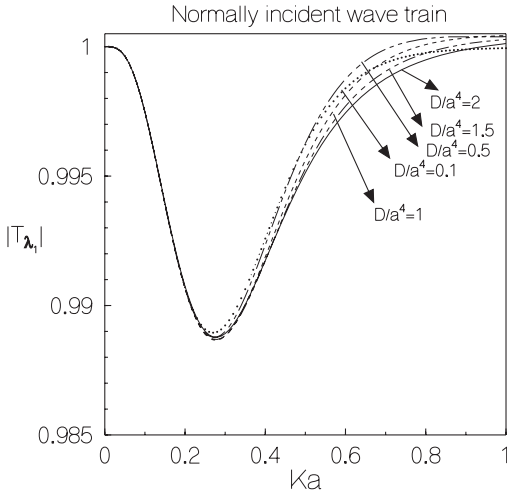

Fig. 11. Transmission coefficient due to a wave of wavenumber λ_1 incident on a cylinder in the lower layer ($\varepsilon/a = 0.01$, $h/a = -2$, $\rho = 0.5$, $f/a = -2$).

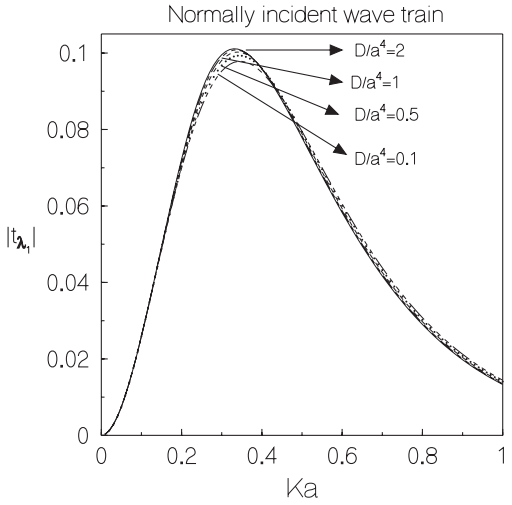

Fig. 12. Transmission coefficient due to a wave of wavenumber λ_1 incident on a cylinder in the lower layer ($\varepsilon/a = 0.01$, $h/a = 2$, $\rho = 0.5$, $f/a = -2$).

where

$$A_n^{(j)}(k) = \frac{1}{2}[\{v(Dv^4 + 1 - \epsilon K) + K\}e^{-vh}\{(-1)^{n+j+1}((1-\rho)v - (1+\rho)K)e^{vf} - (1-\rho)(v-K)e^{-vf}\}]/H(v), \tag{4.5}$$

$$B_n^{(j)}(k) = \frac{1}{2}[(-1)^{n+j+1}\{v(Dv^4 + 1 - \epsilon K) + K\}(1-\rho)(v-K)e^{v(f-h)} - (1-\rho)(v-K)\{v(Dv^4 + 1 - \epsilon K) - K\}e^{-v(f-h)}]/H(v), \tag{4.6}$$

$$C_n^{(j)}(k) = -\rho K[(-1)^{n+j+1}\{v(Dv^4 + 1 - \epsilon K) + K\}e^{v(f-h)} - \{v(Dv^4 + 1 - \epsilon K) - K\}e^{-v(f-h)}]/H(v), \quad j = 0, 1 \tag{4.7}$$

where the contour is indented below the poles $k = \mu_1$ and $k = \mu_2$ in the complex k-plane.

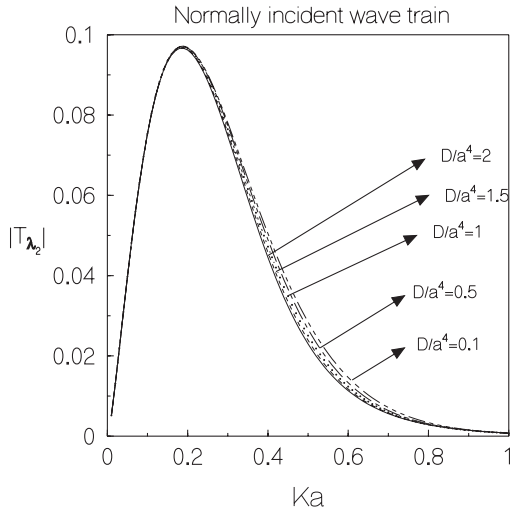

Fig. 13. Transmission coefficient due to a wave of wavenumber λ_2 incident on a cylinder in the lower layer ($\varepsilon/a = 0.01$, $h/a = 2$, $\rho = 0.5$, $f/a = -2$).

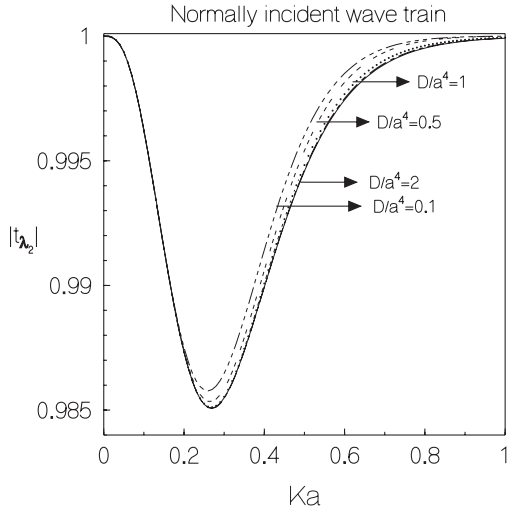

Fig. 14. Transmission coefficient due to a wave of wavenumber λ_2 incident on a cylinder in the lower layer ($\varepsilon/a = 0.01$, $h/a = 2$, $\rho = 0.5$, $f/a = -2$).

The far-field form of these multipoles, in the lower fluid layer, is given by

$$\phi_n^{\mathrm{IIs}} \sim \pi \mathrm{i}(C_n^{(0)\mu_1} \cosh n\mu_1 \mathrm{e}^{\pm \mathrm{i}\beta_1 x + \lambda_1 y} + C_n^{(0)\mu_2} \cosh n\mu_2 \mathrm{e}^{\pm \mathrm{i}\beta_2 x + \lambda_2 y}), \tag{4.8}$$

$$\phi_n^{\mathrm{IIa}} \sim \pm\pi(C_n^{(1)\mu_1} \sinh n\mu_1 \mathrm{e}^{\pm \mathrm{i}\beta_1 x + \lambda_1 y} + C_n^{(1)\mu_2} \sinh n\mu_2 \mathrm{e}^{\pm \mathrm{i}\beta_2 x + \lambda_2 y}), \tag{4.9}$$

as $x \to \pm\infty$, where $C_n^{(j)\mu_1}$ and $C_n^{(j)\mu_2} (j = 0, 1)$ are the residues of $C_n^{(j)}(k)$ at $k = \mu_1$ and $k = \mu_2$, given by

$$C_n^{(j)\mu_i} = -\rho K[(-1)^{n+j+1}\{\lambda_i(D\lambda_i^4 + 1 - \epsilon K) + K\}\mathrm{e}^{\lambda_i(f-h)} - \{\lambda_i(D\lambda_i^4 + 1 - \epsilon K) - K\}\mathrm{e}^{-\lambda_i(f-h)}]/\beta_i H'(\lambda_i),$$
$$i = 1, 2, \quad j = 0, 1. \tag{4.10}$$

The polar expansions of the multipoles, similar to the case when cylinder is in the lower fluid, are

$$\phi_n^{\mathrm{Is}} = K_n(\gamma r)\cos n\theta + \sum_{m=0}^{\infty} B_{nm}^{(s)} I_m(\gamma r)\cos m\theta, \tag{4.11}$$

$$\phi_n^{\mathrm{Ia}} = K_n(\gamma r)\sin n\theta + \sum_{m=1}^{\infty} B_{nm}^{(a)} I_m(\gamma r)\sin m\theta, \tag{4.12}$$

where

$$B_{nm}^{(s)} = \epsilon_m \int_0^{\infty} \cosh mk \cosh nk\{(-1)^m A_n^{(0)}(k)\mathrm{e}^{vf} + B_n^{(0)}(k)\mathrm{e}^{-vf}\}\,\mathrm{d}k, \tag{4.13}$$

$$B_{nm}^{(a)} = 2\int_0^{\infty} \sinh mk \sinh nk\{(-1)^{m+1} A_n^{(1)}(k)\mathrm{e}^{vf} + B_n^{(1)}(k)\mathrm{e}^{-vf}\}\,\mathrm{d}k. \tag{4.14}$$

4.1. Obliquely incident wave train of wavenumber λ_1

For this problem $\phi_{\mathrm{inc}}^{\mathrm{I}}$ is given, in the upper fluid, by $\mathrm{e}^{\mathrm{i}\beta_1 x} g_1(y)$, where $g_1(y)$ is defined in (2.12). The polar expansion of $\phi_{\mathrm{inc}}^{\mathrm{I}}$ is given by

$$\begin{aligned}\phi_{\mathrm{inc}}^{\mathrm{I}} = {} & \sum_{m=0}^{\infty} \epsilon_m I_m(\gamma r)[(-1)^m M_1 \mathrm{e}^{-\lambda_1(h-f)} + M_2 \mathrm{e}^{\lambda_1(h-f)}]\cosh mv \cos m\theta \\ & + \mathrm{i}\sum_{m=0}^{\infty} \epsilon_m I_m(\gamma r)[(-1)^{m+1} M_1 \mathrm{e}^{-\lambda_1(h-f)} + M_2 \mathrm{e}^{\lambda_1(h-f)}]\sin mv \sin m\theta,\end{aligned} \tag{4.15}$$

where

$$\cosh v = \frac{\lambda_1}{\gamma} = \frac{1}{\sin\alpha},$$

and

$$M_{1,2} = \frac{\{(1-\rho)\lambda_1 - K\}\{\lambda_1(D\lambda_1^4 + 1 - \epsilon K) \pm K\}}{K\rho\{\lambda_1(D\lambda_1^4 + 1 - \epsilon K)\cosh\lambda_1 h - K\sinh\lambda_1 h\}}. \tag{4.16}$$

The velocity potential $\phi_{\lambda_1}^{\mathrm{I}}$ is expanded similar as (3.20), where ϕ_n^{s} and ϕ_n^{a} are the symmetric and antisymmetric multipoles developed for the upper fluid, respectively. After applying the body boundary condition, $\frac{\partial \phi_{\lambda_1}^{\mathrm{I}}}{\partial r} = 0$ on $r = a$ and also using the orthogonal properties of trigonometric functions, we obtain the two infinite system of linear equations

$$\frac{a_m}{Z_m} + \sum_{n=1}^{\infty} B_{nm}^{(a)} a_n = 2\mathrm{i}[(-1)^m M_1 \mathrm{e}^{-\lambda_1(h-f)} - M_2 \mathrm{e}^{\lambda_1(h-f)}]\sinh mv, \quad m = 1, 2, \ldots, \tag{4.17}$$

$$\frac{b_m}{Z_m} + \sum_{n=0}^{\infty} B_{nm}^{(s)} b_n = \epsilon_m[(-1)^{m+1} M_1 \mathrm{e}^{-\lambda_1(h-f)} - M_2 \mathrm{e}^{\lambda_1(h-f)}]\cosh mv, \quad m = 0, 1, \ldots. \tag{4.18}$$

These equations were solved by truncations to 5×5 systems to produce the numerical results. The reflection and transmission coefficients can be extracted from the far-field form of the potential $\phi_{\lambda_1}^{\mathrm{I}}$, using (3.20), (4.8) and (4.9) with (3.23), and are given by

$$R_{\lambda_1} = \pi \sum_{m=0}^{\infty} \{ \mathrm{i} b_m C_n^{(0)\mu_1} \cosh m\mu_1 - a_m C_n^{(1)\mu_1} \sinh m\mu_1 \}, \tag{4.19}$$

$$r_{\lambda_1} = \pi \sum_{m=0}^{\infty} \{ \mathrm{i} b_m C_n^{(0)\mu_2} \cosh m\mu_2 - a_m C_n^{(1)\mu_2} \sinh m\mu_2 \}, \tag{4.20}$$

$$T_{\lambda_1} = 1 + \pi \sum_{m=0}^{\infty} \{ \mathrm{i} b_m C_n^{(0)\mu_1} \cosh m\mu_1 + a_m C_n^{(1)\mu_1} \sinh m\mu_1 \}, \tag{4.21}$$

$$t_{\lambda_1} = \pi \sum_{m=0}^{\infty} \{ \mathrm{i} b_m C_n^{(0)\mu_2} \cosh m\mu_2 + a_m C_n^{(1)\mu_2} \sinh m\mu_2 \}. \tag{4.22}$$

4.2. Obliquely incident wave train of wavenumber λ_2

For this problem $\phi^{\mathrm{I}}_{\mathrm{inc}}$ is given, in the upper fluid, by $\mathrm{e}^{\mathrm{i}\beta_2 x} g_2(y)$, where $g_2(y)$ is defined in (2.12). The polar expansion of $\phi^{\mathrm{I}}_{\mathrm{inc}}$ is same as (4.15), except that λ_1 is replaced by λ_2. The velocity potential $\phi^{\mathrm{I}}_{\lambda_2}$ for this scattering problem can again be expanded in multipoles similar to (3.20) and the equations for a_n and b_n are similar to (4.17) and (4.18) with λ_1 replaced by λ_2.

The reflection and transmission coefficients can be extracted from the far-field form of the potential $\phi^{\mathrm{I}}_{\lambda_2}$ using (3.20), (4.8) and (4.9) with (3.28). The expressions for R_{λ_2} and r_{λ_2} are similar to (4.19) and (4.20) with appropriate changes, and the transmission coefficients are given by

$$T_{\lambda_2} = \pi \sum_{m=0}^{\infty} \{ \mathrm{i} b_m C_n^{(0)\mu_1} \cosh m\mu_1 + a_m C_n^{(1)\mu_1} \sinh m\mu_1 \}, \tag{4.23}$$

$$t_{\lambda_2} = 1 + \pi \sum_{m=0}^{\infty} \{ \mathrm{i} b_m C_n^{(0)\mu_2} \cosh m\mu_2 + a_m C_n^{(1)\mu_2} \sinh m\mu_2 \}. \tag{4.24}$$

4.3. Normally incident wave train

Now for the case of normal incidence, $\alpha = 0$, the modified Helmholtz equation reduces to the Laplace's equation and solutions of Laplace's equation singular at $y = f > 0$ are $r^{-n}\cos n\theta$ and $r^{-n}\sin n\theta$, $n \geqslant 1$, and these have the integral representations

$$\frac{\cos n\theta}{r^n} = \frac{1}{(n-1)!} \int_0^{\infty} k^{n-1} \mathrm{e}^{k(y-f)} \cos kx \, \mathrm{d}k,$$

$$\frac{\sin n\theta}{r^n} = \frac{1}{(n-1)!} \int_0^{\infty} k^{n-1} \mathrm{e}^{k(y-f)} \sin kx \, \mathrm{d}k.$$

Here the appropriate multipoles have the forms

$$\phi_n^{\mathrm{Is}} = \frac{\cos n\theta}{r^n} + \frac{1}{(n-1)!} \int_0^{\infty} k^{n-1} (A_n^{(0)}(k)\mathrm{e}^{ky} + B_n^{(0)}(k)\mathrm{e}^{-ky}) \cos kx \, \mathrm{d}k, \tag{4.25}$$

$$\phi_n^{\mathrm{IIs}} = \frac{1}{(n-1)!} \int_0^{\infty} k^{n-1} C_n^{(0)}(k)\mathrm{e}^{ky} \cos kx \, \mathrm{d}k, \tag{4.26}$$

$$\phi_n^{\mathrm{Ia}} = \frac{\sin n\theta}{r^n} + \frac{1}{(n-1)!} \int_0^{\infty} k^{n-1} (A_n^{(1)}(k)\mathrm{e}^{ky} + B_n^{(1)}(k)\mathrm{e}^{-ky}) \sin kx \, \mathrm{d}k, \tag{4.27}$$

$$\phi_n^{\mathrm{IIa}} = \frac{1}{(n-1)!} \int_0^{\infty} k^{n-1} C_n^{(1)}(k)\mathrm{e}^{ky} \sin kx \, \mathrm{d}k, \tag{4.28}$$

where

$$A_n^{(j)}(k) = \frac{1}{2}[\{k(Dk^4 + 1 - \epsilon K) + K\}e^{-kh}\{(-1)^{n+j+1}((1-\rho)k - (1+\rho)K)e^{kf} - (1-\rho)(k-K)e^{-kf}\}]/H(k), \tag{4.29}$$

$$B_n^{(j)}(k) = \frac{1}{2}[(-1)^{n+j+1}\{k(Dk^4 + 1 - \epsilon K) + K\}(1-\rho)(k-K)e^{k(f-h)} - (1-\rho)(k-K)\{k(Dk^4 + 1 - \epsilon K) - K\}e^{-k(f-h)}]/H(k), \tag{4.30}$$

$$C_n^{(j)}(k) = -\rho K[(-1)^{n+j+1}\{k(Dk^4 + 1 - \epsilon K) + K\}e^{k(f-h)} - \{k(Dk^4 + 1 - \epsilon K) - K\}e^{-k(f-h)}]/H(k), \quad j = 0, 1, \tag{4.31}$$

the contour being indented below the poles $k = \lambda_1$ and $k = \lambda_2$ in the complex k-plane.

The polar expansions of these multipoles, in the upper layer, valid for $r < f$, are

$$\phi_n^{\mathrm{Is}} = \frac{\cos n\theta}{r^n} + \sum_{m=0}^{\infty} E_{nm}^{(s)} r^m \cos m\theta, \tag{4.32}$$

$$\phi_n^{\mathrm{Ia}} = \frac{\sin n\theta}{r^n} + \sum_{m=1}^{\infty} E_{nm}^{(a)} r^m \sin m\theta, \tag{4.33}$$

where

$$E_{nm}^{(s)} = \frac{1}{(n-1)!m!}\int_0^{\infty} k^{m+n-1}\{(-1)^m A_n^{(0)}(k)e^{kf} + B_n^{(0)}(k)e^{-kf}\}\,\mathrm{d}k, \tag{4.34}$$

$$E_{nm}^{(a)} = \frac{1}{(n-1)!m!}\int_0^{\infty} k^{m+n-1}\{(-1)^{m+1} A_n^{(1)}(k)e^{kf} + B_n^{(1)}(k)e^{-kf}\}\,\mathrm{d}k. \tag{4.35}$$

We note that unlike the case of multipoles singular in the lower layer, the coefficients in the polar expansions of ϕ_n^{Is} and ϕ_n^{Ia} are not the same.

The far-field behavior of these multipoles, in the lower layer fluid, is given by

$$\phi_n^{\mathrm{IIs}} \sim \frac{\pi \mathrm{i}}{(n-1)!}(\lambda_1^{n-1} C_n^{(0)\lambda_1} e^{\pm \mathrm{i}\lambda_1 x + \lambda_1 y} + \lambda_2^{n-1} C_n^{(0)\lambda_2} e^{\pm \mathrm{i}\lambda_2 x + \lambda_2 y}), \tag{4.36}$$

$$\phi_n^{\mathrm{IIa}} \sim \pm\frac{\pi}{(n-1)!}(\lambda_1^{n-1} C_n^{(1)\lambda_1} e^{\pm \mathrm{i}\lambda_1 x + \lambda_1 y} + \lambda_2^{n-1} C_n^{(1)\lambda_2} e^{\pm \mathrm{i}\lambda_2 x + \lambda_2 y}), \tag{4.37}$$

as $x \to \pm\infty$, where $C_n^{(0)\lambda_1}$ and $C_n^{(1)\lambda_1}$ are the residues of $C_n^{(0)}(k)$ and $C_n^{(1)}(k)$ at $k = \lambda_1$ and $k = \lambda_2$, respectively, and are given by

$$C_n^{(j)\lambda_i} = -\rho K[(-1)^{n+j+1}\{\lambda_i(D\lambda_i^4 + 1 - \epsilon K) + K\}e^{\lambda_i(f-h)} - \{\lambda_i(D\lambda_i^4 + 1 - \epsilon K) - K\}e^{-\lambda_i(f-h)}]/H'(\lambda_i), \quad i = 1, 2,\ j = 0, 1. \tag{4.38}$$

4.4. Normally incident wave train of wavenumber λ_1

For this case $\phi_{\mathrm{inc}}^{\mathrm{I}}$ is given, in the upper fluid, by $e^{\mathrm{i}\lambda_1 x} g_1(y)(\alpha = 0)$, where $g_1(y)$ is defined in (2.12). The polar expansion of $\phi_{\mathrm{inc}}^{\mathrm{I}}$ is given by

$$\phi^{\mathrm{I}}_{\mathrm{inc}} = \sum_{m=0}^{\infty} \frac{(\lambda_1 r)^m}{m!} [\{(-1)^m M_1 \mathrm{e}^{-\lambda_1(h-f)} + M_2 \mathrm{e}^{\lambda_1(h-f)}\} \cosh m\theta + \mathrm{i}\{(-1)^{m+1} M_1 \mathrm{e}^{-\lambda_1(h-f)} + M_2 \mathrm{e}^{\lambda_1(h-f)}\} \sin m\theta], \tag{4.39}$$

where

$$M_{1,2} = \frac{\{(1-\rho)\lambda_1 - K\}\{\lambda_1(D\lambda_1^4 + 1 - \epsilon K) \pm K\}}{K\rho\{\lambda_1(D\lambda_1^4 + 1 - \epsilon K)\cosh \lambda_1 h - K \sinh \lambda_1 h\}}. \tag{4.40}$$

To solve this scattering problem, the velocity potential $\phi^{\mathrm{I}}_{\lambda_1}$ is expanded as in (3.20), where ϕ^{s}_n and ϕ^{a}_n are symmetric and antisymmetric multipoles obtained for the upper fluid. After applying the body boundary condition, $\frac{\partial \phi^{\mathrm{I}}_{\lambda 1}}{\partial r} = 0$ on $r = a$, and using the orthogonal properties of trigonometric functions, we obtain the two infinite system of linear equations for unknown a_n and b_n given by

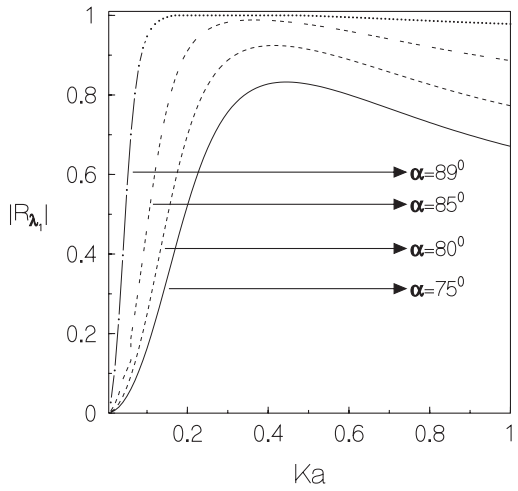

Fig. 15. Reflection coefficient due to a wave of wavenumber λ_1 incident on a cylinder in the upper layer ($D/a^4 = 1.5$, $\varepsilon/a = 0.01$, $h/a = 2.5$, $\rho = 0.5$, $f/a = 1.25$).

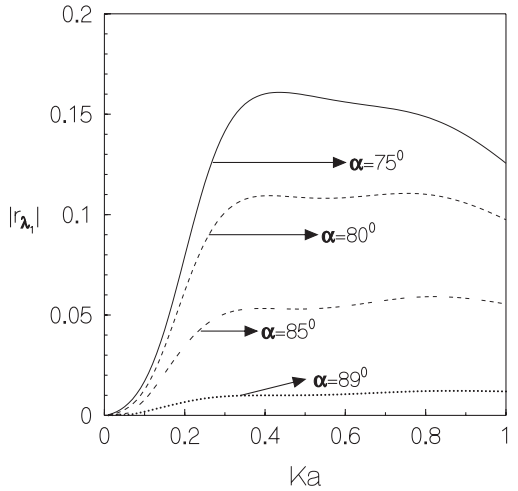

Fig. 16. Reflection coefficient due to a wave of wavenumber λ_1 incident on a cylinder in the upper layer ($D/a^4 = 1.5$, $\varepsilon/a = 0.01$, $h/a = 2.5$, $\rho = 0.5$, $f/a = 1.25$).

$$a_m - \sum_{n=1}^{\infty} a^{n+m} E_{nm}^{(a)} a_n = \mathrm{i}\frac{(\lambda_1 a)^m}{m!}[(-1)^{m+1} M_1 \mathrm{e}^{-\lambda_1(h-f)} + M_2 \mathrm{e}^{\lambda_1(h-f)}], \quad m = 1, 2, \ldots, \tag{4.41}$$

$$b_m - \sum_{n=1}^{\infty} a^{n+m} E_{nm}^{(s)} b_n = \frac{(\lambda_1 a)^m}{m!}[(-1)^m M_1 \mathrm{e}^{-\lambda_1(h-f)} + M_2 \mathrm{e}^{\lambda_1(h-f)}], \quad m = 1, 2, \ldots. \tag{4.42}$$

These equations were solved by truncating to 4×4 system to produce the result presented below.

The reflection and transmission coefficients can be obtained from the far-field form of the potential $\phi_{\lambda_1}^{\mathrm{I}}$, using (3.20), (4.36) and (4.37) with (3.52), and are given by

$$R_{\lambda_1} = \pi \sum_{n=1}^{\infty} \frac{a^n}{(n-1)!} \lambda_1^{n-1}[-a_n C_n^{(1)\lambda_1} + \mathrm{i} b_n C_n^{(0)\lambda_1}], \tag{4.43}$$

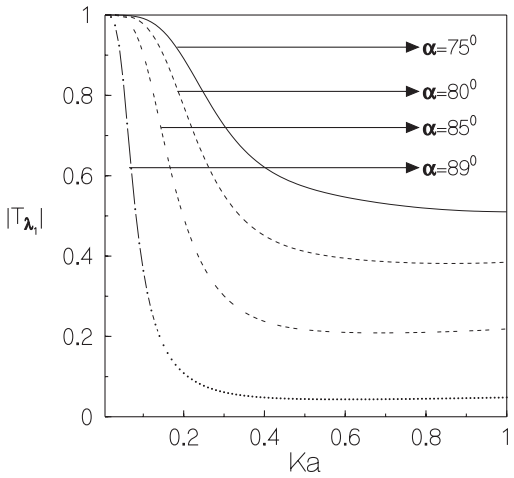

Fig. 17. Transmission coefficient due to a wave of wavenumber λ_1 incident on a cylinder in the upper layer ($D/a^4 = 1.5$, $\varepsilon/a = 0.01$, $h/a = 2.5$, $\rho = 0.5$, $f/a = 1.25$).

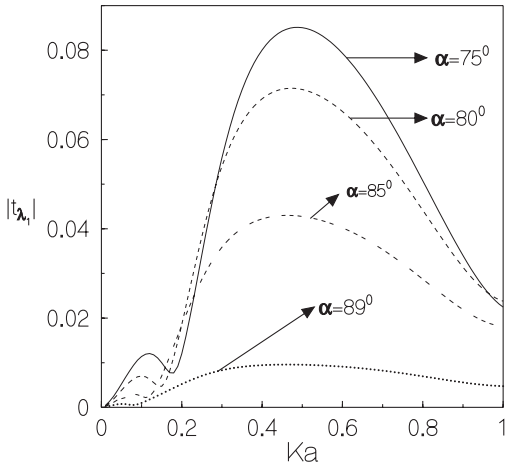

Fig. 18. Transmission coefficient due to a wave of wavenumber λ_1 incident on a cylinder in the upper layer ($D/a^4 = 1.5$, $\varepsilon/a = 0.01$, $h/a = 2.5$, $\rho = 0.5$, $f/a = 1.25$).

$$r_{\lambda_1} = \pi \sum_{n=1}^{\infty} \frac{a^n}{(n-1)!} \lambda_2^{n-1} [-a_n C_n^{(1)\lambda_2} + \mathrm{i} b_n C_n^{(0)\lambda_2}], \tag{4.44}$$

$$T_{\lambda_1} = 1 + \pi \sum_{n=1}^{\infty} \frac{a^n}{(n-1)!} \lambda_1^{n-1} [a_n C_n^{(1)\lambda_1} + \mathrm{i} b_n C_n^{(0)\lambda_1}], \tag{4.45}$$

$$t_{\lambda_1} = \pi \sum_{n=1}^{\infty} \frac{a^n}{(n-1)!} \lambda_2^{n-1} [a_n C_n^{(1)\lambda_2} + \mathrm{i} b_n C_n^{(0)\lambda_2}]. \tag{4.46}$$

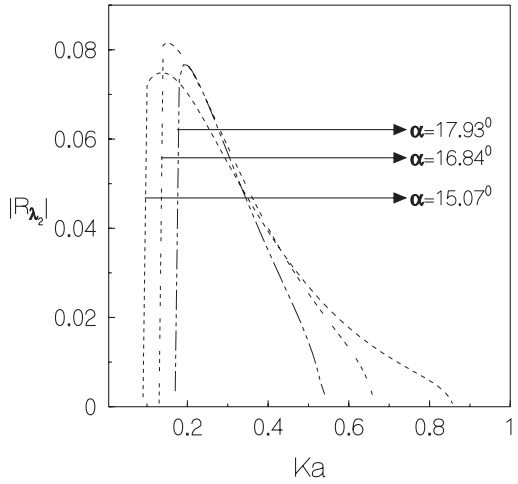

Fig. 19. Reflection coefficient due to a wave of wavenumber λ_2 incident on a cylinder in the upper layer ($D/a^4 = 1.5$, $\varepsilon/a = 0.01$, $h/a = 2.5$, $\rho = 0.5$, $f/a = 1.25$).

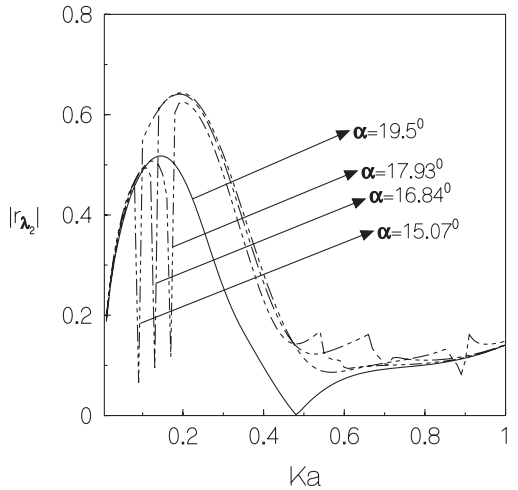

Fig. 20. Reflection coefficient due to a wave of wavenumber λ_2 incident on a cylinder in the upper layer ($D/a^4 = 1.5$, $\varepsilon/a = 0.01$, $h/a = 2.5$, $\rho = 0.5$, $f/a = 1.25$).

4.5. Normally incident wave train of wavenumber λ_2

In this case $\phi^{\mathrm{I}}_{\mathrm{inc}}$ is given by $\mathrm{e}^{\mathrm{i}\lambda_2 x} g_2(y)(\alpha = 0)$, where $g_2(y)$ is defined in (2.12). Here we find that the expressions for reflection coefficients R_{λ_2} and r_{λ_2} are similar to (4.43) and (4.44) with appropriate changes, and the transmission coefficients T_{λ_2} and t_{λ_2} are given by

$$T_{\lambda_2} = \pi \sum_{n=1}^{\infty} \frac{a^n}{(n-1)!} \lambda_1^{n-1} [a_n C_n^{(1)\lambda_1} + \mathrm{i} b_n C_n^{(0)\lambda_1}], \tag{4.47}$$

$$t_{\lambda_2} = 1 + \pi \sum_{n=1}^{\infty} \frac{a^n}{(n-1)!} \lambda_2^{n-1} [a_n C_n^{(1)\lambda_2} + \mathrm{i} b_n C_n^{(0)\lambda_2}]. \tag{4.48}$$

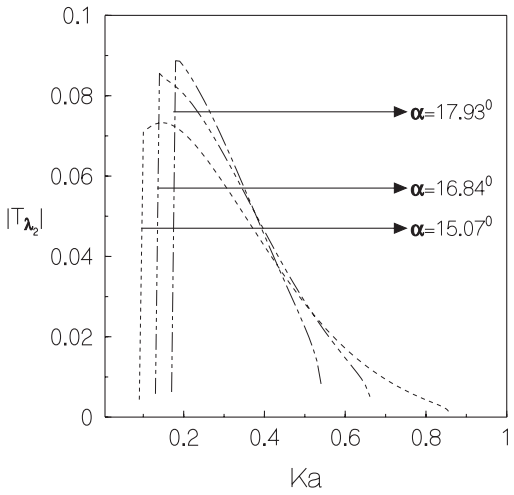

Fig. 21. Transmission coefficient due to a wave of wavenumber λ_2 incident on a cylinder in the upper layer ($D/a^4 = 1.5$, $\varepsilon/a = 0.01$, $h/a = 2.5$, $\rho = 0.5$, $f/a = 1.25$).

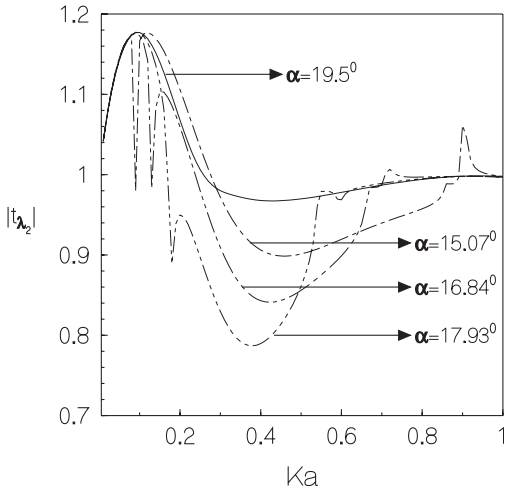

Fig. 22. Transmission coefficient due to a wave of wavenumber λ_2 incident on a cylinder in the upper layer ($D/a^4 = 1.5$, $\varepsilon/a = 0.01$, $h/a = 2.5$, $\rho = 0.5$, $f/a = 1.25$).

4.6. Numerical results

Figs. 15–18 show the reflection and transmission coefficients for an incident wave of wave number λ_1 on a cylinder submerged in the upper fluid layer for $D/a^4 = 1.5$, $\epsilon/a = 0.01$, $h/a = 2.5$, $\rho = 0.5$, $f/a = 1.25$. The different curves correspond to $\alpha = 75°, 80°, 85°, 89°$. The curve are somewhat similar to those for scattering of an incident wave of wave number λ_1 by a circular cylinder in the lower fluid layer and display the same characteristics.

The case of an incident wave of wave number λ_2 is more interesting due to the presence of cut-off frequencies. Figs. 19–22 show reflection coefficients $|R_{\lambda_2}|, |r_{\lambda_2}|$ and transmission coefficients $|T_{\lambda_2}|, |t_{\lambda_2}|$ against Ka. The different parameters are taken to be the same as in the previous set of figures and the different curves correspond to different values of α, viz. $\alpha = 15.07°, 16.84°, 17.93°, 19.5°$. When $\alpha = 19.5°$, which is greater than the critical angle $\alpha_c = 19.13°$, for the given value of different parameters, there are no waves of wave number λ_1

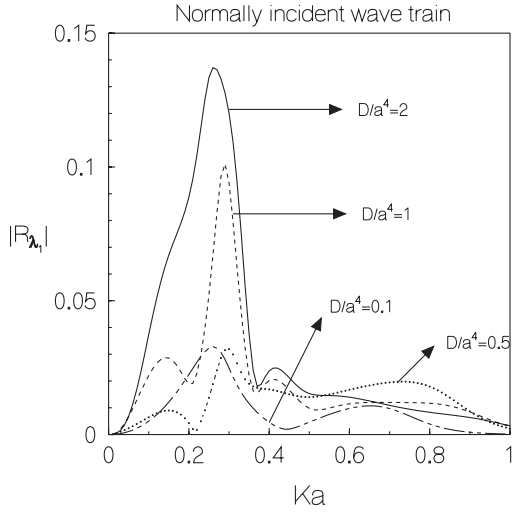

Fig. 23. Reflection coefficient due to a wave of wavenumber λ_1 incident on a cylinder in the upper layer ($\varepsilon/a = 0.01$, $h/a = 2.5$, $\rho = 0.5$, $f/a = 1.25$).

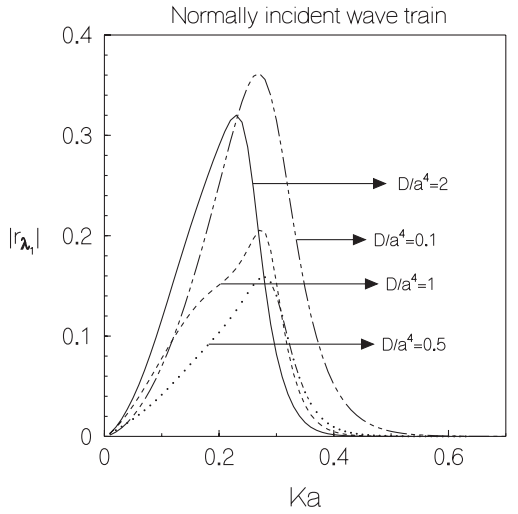

Fig. 24. Reflection coefficient due to a wave of wavenumber λ_1 incident on a cylinder in the upper layer ($\varepsilon/a = 0.01$, $h/a = 2.5$, $\rho = 0.5$, $f/a = 1.25$).

propagating in the fluid. Here we have the following cut-off frequencies: $K_c a = (0.1, 0.88); (0.15, 0.7); (0.2, 0.57)$ corresponding to the incident angles 15.07°, 16.84°, 17.93°, respectively. For these angles and for frequencies lying between two appropriate cut-off frequencies will there be conversion of energy from one mode to the other. These figures are shown in Figs. 19 and 21. The reflection coefficient $|r_{\lambda_2}|$ and transmission coefficient $|t_{\lambda_2}|$ for the wave of wave number λ_2 are shown in Figs. 20 and 22.

We observe from the curves of reflection and transmission coefficients for wave of wave number λ_2 that two spikes in each curve occur at the cut-off frequencies (cf. Figs. 20 and 22). For $\alpha = 19.5°$ which is greater than the critical angle $\alpha_c = 19.13°$, there is no spike in the curves of reflection and transmission coefficients in Figs. 20 and 22.

For the normally incident wave train, we choose $\epsilon/a = 0.01$, $h/a = 2.5$, $\rho = 0.5$, $f/a = 1.25$ for which the reflection and transmission coefficients due to an incident wave of wave number λ_1 are depicted in Figs. 23–26. The different curves correspond to $D/a^4 = 0.1, 0.5, 1, 2$. Figs. 23, 24 and 26 show that the reflection

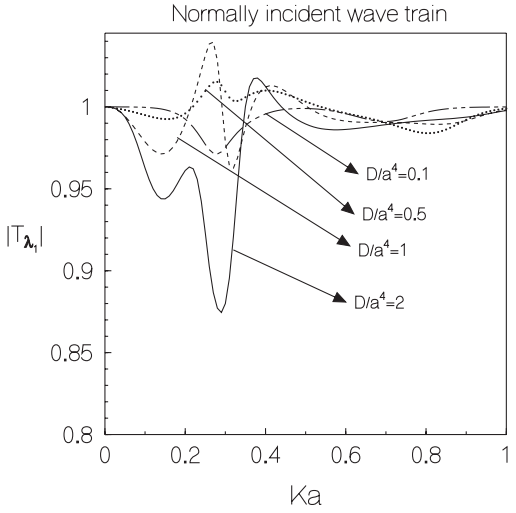

Fig. 25. Transmission coefficient due to a wave of wavenumber λ_1 incident on a cylinder in the upper layer ($\varepsilon/a = 0.01$, $h/a = 2.5$, $\rho = 0.5$, $f/a = 1.25$).

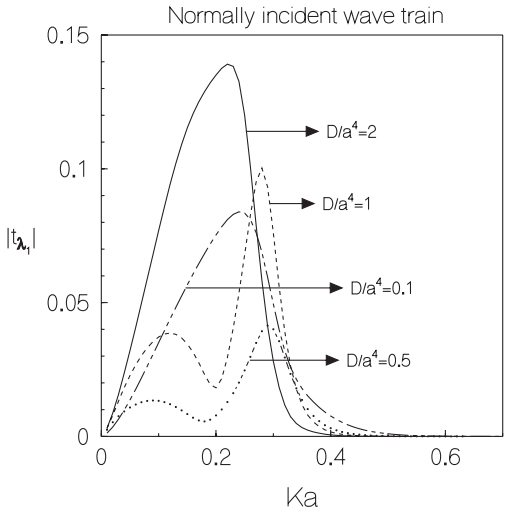

Fig. 26. Transmission coefficient due to a wave of wavenumber λ_1 incident on a cylinder in the upper layer ($\varepsilon/a = 0.01$, $h/a = 2.5$, $\rho = 0.5$, $f/a = 1.25$).

coefficients $|R_{\lambda_1}|$, $|r_{\lambda_1}|$ and the transmission coefficient $|t_{\lambda_1}|$ first increase as Ka increases, each attains a maximum value and then decrease as Ka further increases. Fig. 25 shows that transmission coefficients $|T_{\lambda_1}|$ first decreases as Ka increases, attains a minimum value and then increase as Ka further increases.

The reflection and transmission coefficients due to an incident wave of wave number λ_2 are shown in Figs. 27–30. The different curves correspond to $D/a^4 = 0.1, 0.5, 1, 2$. $|R_{\lambda_2}|, |r_{\lambda_2}|$ are shown in Figs. 27 and 28 and $|T_{\lambda_2}|, |t_{\lambda_2}|$ are shown in Figs. 29 and 30.

Due to the presence of ice-cover, the figures for normally incident wave train are somewhat different from the figures given in the case of upper fluid with a free surface in two-layer fluid by Linton and McIver [3]. Reflection and transmission coefficients due to an incident wave of wave number λ_1 and λ_2 are oscillatory in nature and reflection coefficients for both the incident wave numbers, transmission coefficients $|t_{\lambda_1}|$ and $|T_{\lambda_2}|$ tend ultimately to zero for large Ka and also $|T_{\lambda_1}|$ and $|t_{\lambda_2}|$ tend to unity for large Ka. This may be attributed due to interactions of the incident wave trains between the boundary of the circular cylinder, ice-cover

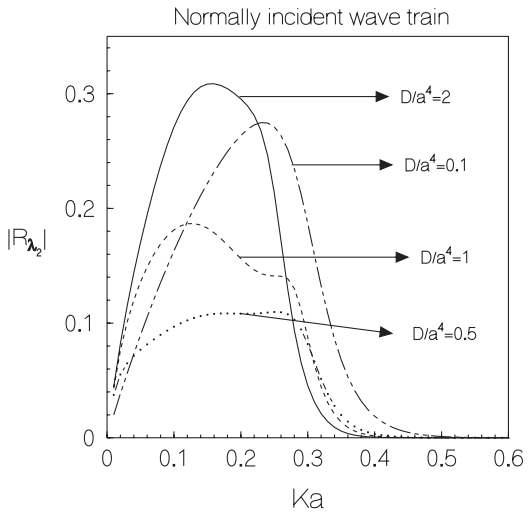

Fig. 27. Reflection coefficient due to a wave of wavenumber λ_2 incident on a cylinder in the upper layer ($\varepsilon/a = 0.01$, $h/a = 2.5$, $\rho = 0.5$, $f/a = 1.25$).

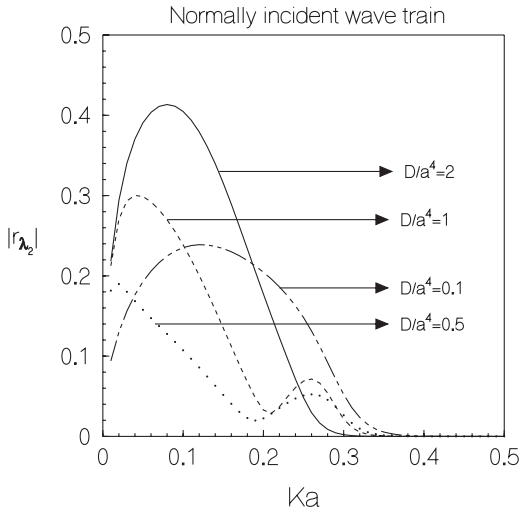

Fig. 28. Reflection coefficient due to a wave of wavenumber λ_2 incident on a cylinder in the upper layer ($\varepsilon/a = 0.01$, $h/a = 2.5$, $\rho = 0.5$, $f/a = 1.25$).

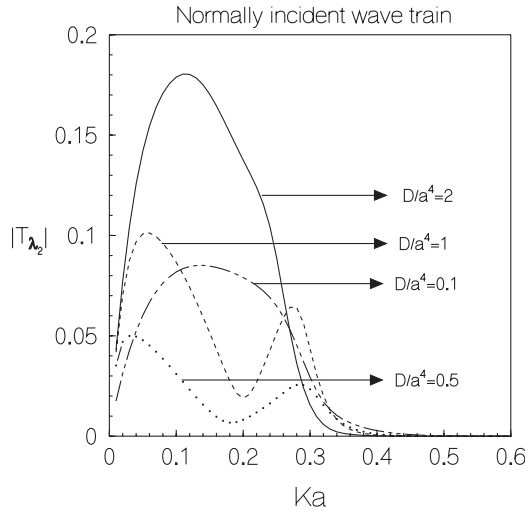

Fig. 29. Transmission coefficient due to a wave of wavenumber λ_2 incident on a cylinder in the upper layer ($\varepsilon/a = 0.01$, $h/a = 2.5$, $\rho = 0.5$, $f/a = 1.25$).

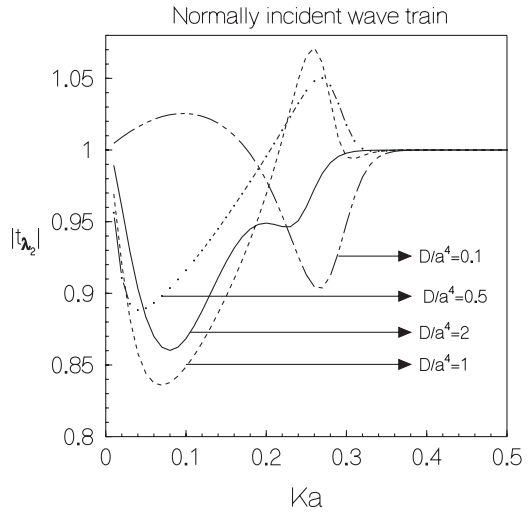

Fig. 30. Transmission coefficient due to a wave of wavenumber λ_2 incident on a cylinder in the upper layer ($\varepsilon/a = 0.01$, $h/a = 2.5$, $\rho = 0.5$, $f/a = 1.25$).

surface and interface between two-layer. Also we observe that the peak values of the curves decrease as D/a^4 decreases in Figs. 23, 24, 26–28 and 29. But in Figs. 25 and 30 the peak value of the curves increase with decreasing D/a^4.

5. Conclusion

In this paper, we have studied the problem of water wave scattering by a horizontal circular cylinder submerged in either layer of a two-layer fluid. The upper layer is of finite depth and is bounded above by an ice-cover modelled as a thin elastic plate and the lower layer extends infinitely downwards. In such a situation propagating waves can exist at two different wave numbers for any frequency, one of which propagates on the ice-cover and the other on the interface. For obliquely incident wave train, and for some values of incident angle two cut-off frequencies are obtained here in contrast to only one cut-off frequency obtained for

a two-layer fluid with free surface. The scattering problem is analyzed for both obliquely and normally incident waves of both the wave numbers using multipole expansions. When the cylinder is positioned in the lower layer and waves are normally incident upon it, it was shown that zero reflections occur for any radius of the cross-section of the cylinder and wave number. When the cylinder is in the upper layer, zero reflection is not observed for normally incident wave train. However, for oblique incidence of the wave train, reflections by the submerged cylinder indeed occur when the cylinder is positioned in either the lower or upper layer fluid. We have found that for oblique waves incident along the interface when a cylinder is in either layer there are isolated frequencies at which almost all the incident energy is reflected. The transmission and reflection coefficients for both obliquely and normally incident wave trains are depicted graphically against the wave number in a number of figures. Energy identities are used as partial numerical checks for all the data points.

Acknowledgment

This work is partially supported by DST through a research project no. SR/S4/MS-263/05.

Appendix A. Derivation of energy identities

Let the boundaries of a finite number of bodies lying in the upper layer be denoted by B_{I} and those in the lower layer by B_{II}. Let ϕ be the solution of a scattering problem with $\phi_n = 0$ on the boundaries B_{I}, B_{II}. The far-field form of ϕ is then given by

$$\phi \sim \{R_{\lambda_1}, r_{\lambda_1}, 1, 0; T_{\lambda_1}, t_{\lambda_1}, 0, 0\} \tag{A.1}$$

for the incident wave of wave number λ_1 and R_{λ_1}, r_{λ_1} are the reflection coefficients of the waves of wave numbers λ_1 and λ_2, respectively, due to an incident wave of wave number λ_1 and similarly T_{λ_1}, t_{λ_1} for the transmission coefficients. Let $\psi = \overline{\phi}$, the complex conjugate of ϕ, then

$$\psi \sim \{1, 0, \overline{R}_{\lambda_1}, \overline{r}_{\lambda_1}; 0, 0, \overline{T}_{\lambda_1}, \overline{t}_{\lambda_1}\}. \tag{A.2}$$

To obtain the energy identity, we use the modified form of Green's integral theorem, as given by

$$\int_S (\phi L_n \psi - \psi L_n \phi) = 0, \tag{A.3}$$

where S denotes the boundary of the fluid region and the differential operator L_n is of the form

$$L_n = D\frac{\partial^5}{\partial n^5} + (1 - \epsilon K)\frac{\partial}{\partial n}, \tag{A.4}$$

$\frac{\partial}{\partial n}$ being the derivative normal to S.

First we choose S in (A.3) to be the boundary of the region in the upper fluid bounded internally by $x = \pm X$, $0 \leqslant y \leqslant h$; $y = h$, $|x| \leqslant X$; $y = 0$, $|x| \leqslant X$ and externally by the body boundary B_{I}, and ultimately make $X \to \infty$, and next to be the boundary of the region in the lower fluid bounded internally by $x = \pm X$, $-Y \leqslant y \leqslant 0$; $y = -Y$, $|x| \leqslant X$; $y = 0$, $|x| \leqslant X$ and externally by the body boundary B_{II}, and ultimately make both $X, Y \to \infty$.

For the upper layer, (A.3) produces

$$\left(\int_{y=h,|x|\leqslant X} + \int_{x=-X,0\leqslant y\leqslant h} + \int_{y=0,|x|\leqslant X} + \int_{x=X,0\leqslant y\leqslant h} + \int_{B_{\mathrm{I}}}\right)(\phi^{\mathrm{I}} L_n \psi^{\mathrm{I}} - \psi^{\mathrm{I}} L_n \phi^{\mathrm{I}})\,\mathrm{d}s = 0. \tag{A.5}$$

The first integral in (A.5) is

$$-\int_{-X}^{X}(\phi^{\mathrm{I}} L_y \psi^{\mathrm{I}} - \psi^{\mathrm{I}} L_y \phi^{\mathrm{I}})(x,h)\,\mathrm{d}x = \int_{-X}^{X}\left[\phi^{\mathrm{I}}\left\{D\left(\frac{\partial^2}{\partial x^2} - \gamma^2\right)^2 + 1 - \epsilon K\right\}\psi_y^{\mathrm{I}} - \psi^{\mathrm{I}}\left\{D\left(\frac{\partial^2}{\partial x^2} - \gamma^2\right)^2 + 1 - \epsilon K\right\}\phi_y^{\mathrm{I}}\right](x,h)\,\mathrm{d}x.$$

Use of the ice-cover condition (2.5) on $y = h$ makes this integral identically equal to zero for any X.

The second integral in (A.5) is

$$\int_0^h (\phi^{\mathrm{I}} L_x \psi^{\mathrm{I}} - \psi^{\mathrm{I}} L_x \phi^{\mathrm{I}})(-X, y)\,\mathrm{d}y.$$

Making use of the far-field behavior of $\phi^{\mathrm{I}}, \psi^{\mathrm{I}}$ for large X, this produces

$$\begin{aligned} &2\mathrm{i}\left[\{D\beta_1^5 + (1-\epsilon K)\beta_1\}(|R_{\lambda_1}|^2 - 1)\int_0^h (g_1(y))^2\,\mathrm{d}y + \{D\beta_2^5 + (1-\epsilon K)\beta_2\} \times |r_{\lambda_1}|^2 \int_0^h (g_2(y))^2\,\mathrm{d}y\right] \\ &\quad + \mathrm{i}[\{D(\beta_1^5 - \beta_2^5) + (1-\epsilon K)(\beta_1 - \beta_2)\}(-r_{\lambda_1}\mathrm{e}^{-\mathrm{i}(\beta_1+\beta_2)X} + \overline{r}_{\lambda_1}\mathrm{e}^{\mathrm{i}(\beta_1+\beta_2)X}) \\ &\quad + \{D(\beta_1^5 + \beta_2^5) + (1-\epsilon K)(\beta_1 + \beta_2)\}(R_{\lambda_1}\overline{r}_{\lambda_1}\mathrm{e}^{-\mathrm{i}(\beta_1-\beta_2)X} + r_{\lambda_1}\overline{R}_{\lambda_1}\mathrm{e}^{\mathrm{i}(\beta_1-\beta_2)X})]\int_0^h g_1(y)g_2(y)\,\mathrm{d}y. \end{aligned} \tag{A.6}$$

Similarly the fourth integral in (A.5) produces

$$\begin{aligned} &2\mathrm{i}\left[\{D\beta_1^5 + (1-\epsilon K)\beta_1\}|T_{\lambda_1}|^2 \int_0^h (g_1(y))^2\,\mathrm{d}y + \{D\beta_2^5 + (1-\epsilon K)\beta_2\}|r_{\lambda_1}|^2 \int_0^h (g_2(y))^2\,\mathrm{d}y\right] \\ &\quad + \mathrm{i}[\{D(\beta_1^5 + \beta_2^5) + (1-\epsilon K)(\beta_1 + \beta_2)\}(T_{\lambda_1}\overline{t}_{\lambda_1}\mathrm{e}^{-\mathrm{i}(\beta_1-\beta_2)X} + t_{\lambda_1}\overline{T}_{\lambda_1}\mathrm{e}^{\mathrm{i}(\beta_1-\beta_2)X})]\int_0^h g_1(y)g_2(y)\,\mathrm{d}y. \end{aligned} \tag{A.7}$$

The third integral in (A.5) is

$$\int_{-X}^{X} (\phi^{\mathrm{I}} L_y \psi^{\mathrm{I}} - \psi^{\mathrm{I}} L_y \phi^{\mathrm{I}})(x, 0)\,\mathrm{d}x. \tag{A.8}$$

Finally, the last integral in (A.5) becomes

$$\int_{B_{\mathrm{I}}} (\phi^{\mathrm{I}} L_n \psi^{\mathrm{I}} - \psi^{\mathrm{I}} L_n \phi^{\mathrm{I}})\,\mathrm{d}s.$$

Let the cross-section B_{I} of the submerged cylinder be described parametrically by $x = X(\theta)$, $y = Y(\theta)$, $0 \leqslant \theta \leqslant 2\pi$ where $\theta = 0$ is chosen to be coincident with the line $x = 0$. Defining (n, s) as rectangular co-ordinates along the normal and tangent to B_{I} at any point of B_{I}, then the functions $\phi^{\mathrm{I}}, \psi^{\mathrm{I}}$ satisfy $(\nabla_1^2 - \gamma^2)\phi^{\mathrm{I}} = 0, (\nabla_1^2 - \gamma^2)\psi^{\mathrm{I}} = 0$ where $\nabla_1^2 = \frac{\partial^2}{\partial s^2} + \frac{\partial^2}{\partial n^2} + \kappa(s)\frac{\partial}{\partial n}$, $\kappa(s)$ being the curvature as a function of the arc length s. We now find that the last integral in (A.5) is

$$\int_{B_{\mathrm{I}}} \left[\phi^{\mathrm{I}}(D\mathscr{M}_s + 1 - \epsilon K)\frac{\partial \psi^{\mathrm{I}}}{\partial n} - \psi^{\mathrm{I}}(D\mathscr{M}_s + 1 - \epsilon K)\frac{\partial \phi^{\mathrm{I}}}{\partial n}\right]\mathrm{d}s = 0, \tag{A.9}$$

after using the conditions $\frac{\partial \phi^{\mathrm{I}}}{\partial n} = 0, \frac{\partial \psi^{\mathrm{I}}}{\partial n} = 0$ on B_{I}, the differential operator $\mathscr{M}_s$ in (A.9) having the form

$$\mathscr{M}_s = \left(\frac{\partial^2}{\partial s^2} - \gamma^2\right)^2 - (\kappa(s))^2\left(\frac{\partial^2}{\partial s^2} - \gamma^2\right) + \left(\kappa''(s) + 2\kappa(s)\left(\frac{\partial^2}{\partial s^2} - \gamma^2\right) - (\kappa(s))^3\right)Q(s)\frac{\partial}{\partial s},$$

$Q(s) = \frac{(Y'(\theta))^2 - (X'(\theta))^2}{X'(\theta)Y'(\theta)}$ being a function of s.

For the lower layer, (A.3) produces

$$\left(\int_{y=0,|x|\leqslant X} + \int_{x=-X,-Y\leqslant y\leqslant 0} + \int_{y=-Y,|x|\leqslant X} + \int_{x=X,-Y\leqslant y\leqslant 0} + \int_{B_{\mathrm{II}}}\right)(\phi^{\mathrm{II}} L_n \psi^{\mathrm{II}} - \psi^{\mathrm{II}} L_n \phi^{\mathrm{II}})\,\mathrm{d}s = 0. \tag{A.10}$$

The first integral in (A.10) is

$$\int_{-X}^{X} (\phi^{\mathrm{II}} L_y \psi^{\mathrm{II}} - \psi^{\mathrm{II}} L_y \phi^{\mathrm{II}})(x, 0)\,\mathrm{d}x. \tag{A.11}$$

The second integral in (A.10) reduces to, after using the far-field behavior of $\phi^{\mathrm{II}}, \psi^{\mathrm{II}}$ for large X,

$$\begin{aligned}&\mathrm{i}\left[\frac{1}{\lambda_1}\{D\beta_1^5+(1-\epsilon K)\beta_1\}(|R_{\lambda_1}|^2-1)+\frac{1}{\lambda_2}\{D\beta_1^5+(1-\epsilon K)\beta_1\}|r_{\lambda_1}|^2\right]\\&\quad+\mathrm{i}[\{D(\beta_1^5-\beta_2^5)+(1-\epsilon K)(\beta_1-\beta_2)\}(-r_{\lambda_1}\mathrm{e}^{-\mathrm{i}(\beta_1+\beta_2)X}+\overline{r}_{\lambda_1}\mathrm{e}^{\mathrm{i}(\beta_1+\beta_2)X})\\&\quad+\{D(\beta_1^5+\beta_2^5)+(1-\epsilon K)(\beta_1+\beta_2)\}(R_{\lambda_1}\overline{r}_{\lambda_1}\mathrm{e}^{-\mathrm{i}(\beta_1-\beta_2)X}+r_{\lambda_1}\overline{R}_{\lambda_1}\mathrm{e}^{\mathrm{i}(\beta_1-\beta_2)X})]\int_{-\infty}^{0}\mathrm{e}^{(\lambda_1+\lambda_2)y}\,\mathrm{d}y.\end{aligned}\tag{A.12}$$

Similarly, the fourth integral in (A.10) reduces to

$$\begin{aligned}&\mathrm{i}\left[\frac{1}{\lambda_1}\{D\beta_1^5+(1-\epsilon K)\beta_1\}|T_{\lambda_1}|^2+\frac{1}{\lambda_2}\{D\beta_1^5+(1-\epsilon K)\beta_1\}|t_{\lambda_1}|^2\right]\\&\quad+\mathrm{i}[\{D(\beta_1^5+\beta_2^5)+(1-\epsilon K)(\beta_1+\beta_2)\}\{T_{\lambda_1}\overline{t}_{\lambda_1}\mathrm{e}^{-\mathrm{i}(\beta_1-\beta_2)X}+t_{\lambda_1}\overline{T}_{\lambda_1}\mathrm{e}^{\mathrm{i}(\beta_1-\beta_2)X}\}]\int_{-\infty}^{0}\mathrm{e}^{(\lambda_1+\lambda_2)y}\,\mathrm{d}y.\end{aligned}\tag{A.13}$$

Again, the third integral in (A.10) tends to 0 as $Y\to-\infty$, after using the conditions at infinite depth.

Finally, the last integral in (A.10) becomes,

$$\int_{B_{\mathrm{II}}}\left[\phi^{\mathrm{II}}(D\mathscr{M}_s+1-\epsilon K)\frac{\partial\psi^{\mathrm{II}}}{\partial n}-\psi^{\mathrm{II}}(D\mathscr{M}_s+1-\epsilon K)\frac{\partial\phi^{\mathrm{II}}}{\partial n}\right]\mathrm{d}s=0,\tag{A.14}$$

after using $\frac{\partial\phi^{\mathrm{II}}}{\partial n}=0$ and $\frac{\partial\psi^{\mathrm{II}}}{\partial n}=0$ on B_{II}.

Substituting all these results in (A.5), (A.10), and multiplying (A.5) by ρ and adding with (A.10) and using the result

$$\rho\left(\phi^{\mathrm{I}}\frac{\partial\psi^{\mathrm{I}}}{\partial y}-\psi^{\mathrm{I}}\frac{\partial\phi^{\mathrm{I}}}{\partial y}\right)=\phi^{\mathrm{II}}\frac{\partial\psi^{\mathrm{II}}}{\partial y}-\psi^{\mathrm{II}}\frac{\partial\phi^{\mathrm{II}}}{\partial y}\tag{A.15}$$

at the interface, we obtain after some algebra which includes the result

$$\rho\int_0^h g_1(y)g_2(y)\mathrm{d}y+\int_{-\infty}^{0}\mathrm{e}^{(\lambda_1+\lambda_2)y}\,\mathrm{d}y=0\tag{A.16}$$

and after making $X\to\infty$,

$$J_{\beta_1}(|R_{\lambda_1}|^2+|T_{\lambda_1}|^2-1)+J_{\beta_2}(|r_{\lambda_1}|^2+|t_{\lambda_1}|^2)=0,\tag{A.17}$$

where

$$J_{\beta_j}=i(D\beta_j^5+(1-\epsilon K)\beta_j)\left\{\frac{1}{\lambda_j}+2\rho\int_0^h(g_j(y))^2\,\mathrm{d}y\right\},\quad j=1,2.\tag{A.18}$$

Thus we obtain the identity

$$|R_{\lambda_1}|^2+|T_{\lambda_1}|^2+J(|r_{\lambda_1}|^2+|t_{\lambda_1}|^2)=1,\tag{A.19}$$

where

$$J=\frac{J_{\beta_2}}{J_{\beta_1}}.\tag{A.20}$$

Similarly for the scattering of an incident wave of wave number λ_2, we obtain the identity

$$|R_{\lambda_2}|^2+|T_{\lambda_2}|^2+J(|r_{\lambda_2}|^2+|t_{\lambda_2}|^2)=J.\tag{A.21}$$

The relations (A.19) and (A.21) are the *energy identities*.

References

[1] G.G. Stokes, On the theory of oscillatory waves, Trans. Cambridge Philos. Soc. 8 (1847) 441–445, Reprinted in Maths. Phys. papers, Cambridge University Press, vol. 1, 1847, pp. 314–326.
[2] H. Lamb, Hydrodynamics, Cambridge University Press, 1932.
[3] C.M. Linton, M. McIver, The interaction of waves with horizontal cylinders in two-layer fluids, J. Fluid Mech. 304 (1995) 213–229.
[4] F. Ursell, Surface waves on deep water in the presence of a submerged circular cylinder, I–II, Proc. Cambridge Philos. Soc. 46 (1950) 141–152.
[5] C.M. Linton, J.R. Cadby, Scattering of oblique waves in a two-layer fluid, J. Fluid Mech. 461 (2002) 343–364.
[6] C. Fox, V.A. Squire, On the oblique reflection and transmission of ocean waves at shore fast sea ice, Philos. Trans. R. Soc. A 347 (1994) 185–218.
[7] A. Chakrabarti, On the solution of the problem of scattering of surface water waves of the edge of an ice-cover, Proc. R. Soc. Lond. A 456 (2000) 1087–1099.
[8] H. Chung, C. Fox, Calculation of wave–ice interaction using the Wiener–Hopf technique, New Zealand J. Math. 31 (2002) 1–18.
[9] L.A. Tkacheva, Scattering of surface waves by the edge of a floating elastic plate, J. Appl. Math. Tech. Phys. 42 (2001) 638–646.
[10] C.M. Linton, H. Chung, Reflection and transmission at the ocean/sea-ice boundary, Wave Motion 1126 (2003) 1–10.
[11] B.N. Mandal, U. Basu, Wave diffraction by a small elevation of the bottom of an ocean with an ice-cover, Arch. Appl. Mech. 73 (2004) 812–822.
[12] R. Gayen (chowdhury), B.N. Mandal, A. Chakrabarti, Water wave scattering by an ice-strip, J. Eng. Math. 53 (2005) 21–37.
[13] P. Maiti, B.N. Mandal, Water waves generated due to initial axisymmetric disturbances in water with an ice-cover, Arch. Appl. Mech. 74 (2005) 629–636.
[14] Dilip Das, B.N. Mandal, Oblique wave scattering by a circular cylinder submerged beneath an ice-cover, Int. J. Eng. Sci. 44 (2006) 166–179.
[15] Dilip Das, B.N. Mandal, Oblique wave scattering by a circular cylinder in two-layer fluid with an ice-cover, in: 21st IWWWFB, Loughborough University, UK, 2–5 April, 2006, pp. 29–32.